

THESIS

INVESTIGATION OF A NEW MICROCHIP ELECTROPHORESIS INSTRUMENT
FOR SEMI-CONTINUOUS AEROSOL COMPOSITION MEASUREMENTS

Submitted by

Ashley R. Evanoski-Cole

Department of Atmospheric Science

In partial fulfillment of the requirements

For the Degree of Master of Science

Colorado State University

Fort Collins, Colorado

Spring 2012

Master's Committee:

Advisor: Jeffrey L. Collett, Jr.

Charles S. Henry

Sonia M. Kreidenweis

ABSTRACT

INVESTIGATION OF A NEW MICROCHIP ELECTROPHORESIS INSTRUMENT FOR SEMI-CONTINUOUS AEROSOL COMPOSITION MEASUREMENTS

The high variability of atmospheric aerosol composition over both time and space and their importance to the global radiation budget, biogeochemical processes, human health, atmospheric visibility and other important issues has motivated the development of a novel instrument to measure temporal and geographical trends of aerosol composition. The aerosol microchip electrophoresis (ACE) instrument uses a water condensation growth tube to collect water soluble aerosols. Rapid separation and detection of common inorganic ions (chloride, nitrate and sulfate) and one organic acid (oxalate) in the collected aqueous sample is achieved using microchip capillary electrophoresis coupled with conductivity detection. The ACE system was tested in multiple pilot field studies and compared with measurements collected by a particle-into-liquid sampler coupled with an ion chromatograph (PILS-IC) and filter samples. Laboratory tests were also performed with generated aerosol to test the accuracy of ACE. The ACE system has the advantage of being able to achieve fast semi-continuous measurements with time resolution up to one minute. Additionally, the small size footprint and low manufacturing cost make ACE an ideal field instrument to attain rapid and sensitive aerosol composition measurements.

ACKNOWLEDGEMENTS

For being an exceptional mentor, I would like to thank Scott Noblitt, now with Scripps Institution of Oceanography and previously a student in the Department of Chemistry at Colorado State University, for spending many hours teaching me the wily ways of the microchip. As the initial developer and sole expert of the ACE, he provided much instruction, answered countless questions, and helped with a lot of trouble-shooting.

Acknowledgement is also well deserved for Amy Sullivan and Katie Benedict in their expertise of and help with the PILS-IC. Katie provided PILS-IC data collected in Rocky Mountain National Park and Amy assisted in operating the PILS-IC for studies done in the lab. Ezra Levin is also acknowledged for his assistance in setting up an aerosol generation and monitoring system used for the ACE laboratory studies.

Special acknowledgement is also deserved for my advisor, Jeff Collett, for all the guidance he provided during this project and especially for the encouragement when I was dealing with the temperamental nature of a prototype instrument. My committee members, Sonia Kreidenweis and Chuck Henry, were also valuable for all the advice, comments, and assistance so willingly provided.

Collaboration with Aerosol Dynamics, Inc. in this project is acknowledged for the development of the growth tube and fabrication of the microchip box used in ACE.

Lastly, I would like to thank my family and friends, particularly my husband Michael, who have provided support and encouragement all throughout my educational career.

This project was funded by the National Science Foundation grant ATM-0737201.

TABLE OF CONTENTS

	Page
ABSTRACT	ii
ACKNOWLEDGEMENTS	iii
TABLE OF CONTENTS.....	v
LIST OF TABLES	vii
LIST OF FIGURES.....	viii
CHAPTER 1. INTRODUCTION.....	1
1.1 Motivation.....	1
1.1.1 Importance of Studying Atmospheric Aerosol Composition	1
1.1.2 Challenges of Aerosol Measurements and Instrumentation	5
1.2 ACE Instrument Theory	9
1.2.1 Particle Collection with a Growth Tube	10
1.2.2 Separation Using Microchip Capillary Electrophoresis	16
1.2.3 Conductivity Detection Method.....	23
1.3 Previous Measurements with ACE.....	25
CHAPTER 2. MATERIALS, METHODS AND CALCULATIONS	29
2.1 Project Overview	29
2.2 Materials	29
2.3 Methods	30
2.3.1 Microchip Fabrication	30
2.3.2 Standard ACE Operation	34
2.3.3 Instrumentation for Generated Aerosol Experiments.....	35
2.3.4 PILS-IC Operation	35
2.4 Calculations.....	37
2.4.1 Ambient Aerosol Calculation for ACE	37
2.4.2 Sulfate Calculation Using the CPC	39
2.4.3 PILS-IC Calculation	40
2.4.4 Statistical Calculations	41
2.5 Quality Assurance and Quality Control.....	43
CHAPTER 3. RESULTS.....	46

3.1	Instrumental Conditions.....	46
3.2	ACE Comparison Data	48
3.3	Generated Aerosol Experiment	53
CHAPTER 4. INSTRUMENT AND METHOD VALIDATION		57
4.1	Statistical Analysis of ACE Data	57
4.1.1	Instrumental Detection Limits	57
4.1.2	Data Averaging Analysis	58
4.1.3	Variation in Measured Concentrations	60
4.1.4	ACE Calibration.....	63
4.2	Analysis of ACE Ambient Aerosol Calculation	65
4.3	Improvements in ACE	65
CHAPTER 5. DISCUSSION OF FIELD STUDY DATA.....		70
5.1	Description of Field Sites	70
5.2	Comparison of Ambient Aerosol Measurements	73
CHAPTER 6. INSTRUMENT PERFORMANCE IN FIELD OPERATION.....		77
6.1	Instrument Automation and Limitations.....	77
6.2	Challenges of the Electrophoresis Separation.....	80
6.3	Uncertainty Analysis of ACE	83
CHAPTER 7. CONCLUSIONS.....		89
7.1	ACE Field Study Conclusions	89
7.2	ACE Laboratory Study Conclusions	91
CHAPTER 8. FUTURE WORK.....		92
8.1	Future Field Studies.....	92
8.2	Future Laboratory Tests.....	92
8.3	Future Improvements to ACE	93
REFERENCES.....		95

LIST OF TABLES

Table 2.2: The average noise as calculated by averaging the standard deviation of the baseline signal (mV) is shown for the two data files collected over the sampling period. The number of baseline sections used to calculate the average standard deviation is shown in parenthesis.	44
Table 3.1: Average concentration and comparison statistics for sulfate and nitrate concentrations measured in RMNP and FC.	52
Table 3.2: Averaged daily concentrations as measured by the ACE, PILS, and URG systems for the only three full days of ACE data collected during the sampling campaign. In parenthesis are the calculated values of percent difference between the averaged daily concentrations as measured by the ACE system and PILS or URG measurements.	53
Table 3.3: The sulfate concentrations measured by ACE and CPC are listed with the relative 95% confidence interval in the parenthesis.	55
Table 4.1: The calculated ambient aerosol LODs for nitrate and sulfate in ACE are shown as measured in both RMNP and FC.	58
Table 4.2: The averaged relative 95% confidence intervals (RCI) calculated for each 17 minute averaged ACE data point and the relative standard deviation (RSD) for the sulfate and nitrate concentrations as measured by the PILS-IC is shown for each field campaign.	61
Table 4.3: The concentration of each standard (μM) for the sulfate and nitrate calibration curves is listed along with the R^2 value.	63
Table 6.1: The average migration times of sulfate and the internal standard PDS measured during the generated aerosol studies are listed for 50 nm diameter particles with the range in parenthesis.	84
Table 6.2: The average migration times of sulfate, nitrate and PDS collected during the RMNP field campaign are listed with the range of migration times in parenthesis.	85

LIST OF FIGURES

Figure 1.1: A photograph was taken showing the ACE system and the major components were labeled.....	10
Figure 1.2: The typical temperature and saturation profiles formed in the growth tube are shown as a function of axial distance to tube radius (z/R). The wall temperature is also indicated, marking the thermal break in the controlled temperature of the growth tube (Hering et al., 2009).....	11
Figure 1.3: The collection efficiency was measured as a function of particle diameter with varying growth tube temperatures (Hering et al., 2009).....	15
Figure 1.4: A schematic of the growth tube in the ACE system depicts the denuder that removes gases before the ambient sample enters the growth tube, the conditioner and growth region of the growth tube, and the microchip sample reservoir where the particles are impacted.	16
Figure 1.5: The basic design for buffer reservoirs and channels in a microchip is shown. (A) is the sample reservoir, (B) is the buffer reservoir, (C) is the buffer waste reservoir, (D) is the sample waste reservoir and (E) is the detection electrodes.	21
Figure 1.6: The ACE microchip as connected to wires leading to the high voltage supply and ground and the conductivity detector are shown in this photograph. The channels and detection wires are also highlighted.....	22
Figure 1.7: Sulfate (black) and nitrate concentrations (red) were measured by the ACE system (triangles) and compared with a PILS-IC (open circles). The sampling time resolution was 15 minutes for PILS-IC sulfate and nitrate, 5 minutes for ACE nitrate and 3 minutes for ACE sulfate.....	26
Figure 2.1: This photograph shows the most recent microchip design as used in both RMNP and FC field studies.	31
Figure 2.2: The microchip design is shown with labeled reservoirs and all sample channels. The microwires are color coded with red being at a high negative voltage, black at ground and green indicates the detection wires.	32
Figure 2.3: The instrument set up of generated aerosol shown was used to make comparison measurements between the ACE and CPC.	35
Figure 3.1: The concentrations of sulfate and nitrate measured in RMNP from September 17-September 21, 2010 using both the PILS-IC (black line) and the ACE (sulfate in red in the top half and nitrate in blue in the bottom half).....	49
Figure 3.2: The concentrations of sulfate and nitrate measured in Fort Collins from June 17 to June 24 in 2011 using both the PILS-IC (black line) and the ACE (sulfate in red and nitrate in blue)	50
Figure 3.3: The measurements from PILS-IC are compared directly with measurements by ACE for sulfate (a) and nitrate (b). A 1:1 line is plotted as the solid black line.	51

Figure 3.4: The measurements from PILS-IC are compared directly with measurements by ACE for nitrate collected in RMNP with a 1:1 line plotted in solid black.51

Figure 3.5: The sulfate concentration as measured by the ACE instrument are compared to the CPC for 50 nm diameter particles. Error in ACE concentration is represented by 95% confidence interval. The error in the CPC-derived concentration is not observable in this scale.....55

Figure 4.1: Nitrate measurements from PILS-IC (black line) were compared with measurements from ACE averaged an additional two, five and ten times the original 17 minute averaged data set used in Figure 3.2 (green, purple and blue squares and lines, respectively).60

Figure 4.2: The calibration curves for sulfate and nitrate at both RMNP and FC field studies are shown with their linear regression equation.64

Figure 5.1: The sulfate and nitrate concentrations from 24 hour PM2.5 filter samples collected in RMNP during 2011 are displayed (IMPROVE, 2010).71

Figure 5.2: Hourly PM2.5 concentrations as measured by the Colorado Department of Public Health and Environment in Fort Collins at the CSU Facilities site (colorado.gov, 2011).72

Figure 6.1: Over one injection cycle lasting 70 minutes, the ambient sulfate concentration (Caer), sulfate peak to internal standard peak ratio (Pi/Pis) and aqueous sulfate concentration (Cliq) for each 60 second analysis are plotted.86

CHAPTER 1. INTRODUCTION

1.1 Motivation

1.1.1 Importance of Studying Atmospheric Aerosol Composition

Measuring and characterizing atmospheric aerosol particles has been a challenging problem due to the complexity of aerosols which arise from their wide ranges in size, composition, optical properties, and concentration over both time and location. Each aerosol property has varying effects and influences on issues such as the global radiation budget, biogeochemical cycles, visibility and human health. To better understand how to mitigate the undesired effects of anthropogenic aerosol, a range of aerosol instrumentation has been developed and used to gain comprehensive aerosol measurements.

The sizes of aerosol particles can start at just a few nanometers and reach up to tens of micrometers. For regulatory measures and air pollution mitigation, the United States Environmental Protection Agency (USEPA) divides aerosol particles into two different size classes. The size classes include fine particles which have diameters less than $2.5\mu\text{m}$ ($\text{PM}_{2.5}$) and coarse particles which have diameters between 2.5 and $10\mu\text{m}$ (PM_{10}) (U.S. EPA, 2009). This size classification was created based on the adverse human health effects caused by the ability of fine particles to penetrate deep into the lungs. The

National Ambient Air Quality Standards (NAAQS), created by the USEPA, set unhealthy exposure levels of both $PM_{2.5}$ and PM_{10} . Numerous sites throughout the U.S. use instrumentation to monitor $PM_{2.5}$ and PM_{10} concentrations to ensure all sites are in compliance. If the site has higher PM concentrations than the regulations allow, states are required to take action to reduce concentrations to ensure adequate air quality.

The importance of reducing particulate concentrations has been shown in epidemiological studies that have found relationships linking both concentration and exposure length of fine particulates to increased cases of cardio-pulmonary diseases and even increased mortality (Pope and Dockery, 2006; U.S. EPA, 2009). Though conclusive evidence has not been discovered, some epidemiological and toxicology studies suggest that specific aerosol components such as sulfate found in fine particulate matter could have a negative effect on health impacts (Schlesinger, 2007). This lack of conclusive evidence reinforces the need for aerosol composition data to conduct additional health studies.

In addition to $PM_{2.5}$ being the most detrimental particle size to human health, the importance of sample collection at this size range is also justified by the fact that $PM_{2.5}$ contributes a larger number concentration of total particulate matter. The accumulation mode, particles with diameters ranging from 0.1-2.5 μm , is used to describe the larger particles in the fine classification as described above. The name arises from their tendency to accumulate in the atmosphere, thus generating high mass concentrations at this size. Accumulation mode particles are small enough where gravitational settling is negligible and are large enough where condensational growth is also inefficient.

Therefore, the most efficient removal mechanism is wash out from precipitation which causes this size to accumulate in the atmosphere between precipitation events (Seinfeld and Pandis, 2006).

Measuring the composition of water soluble or hygroscopic aerosols is particularly useful in understanding their optical properties which can directly affect their potential to absorb and scatter radiation. Aerosols can either warm or cool the Earth's climate directly or act indirectly to alter the radiation budget. Two proposed mechanisms, termed the first and second indirect effects, describe how aerosols can indirectly affect the atmosphere's radiation budget. The first indirect effect, or Twomey effect, states that with increased aerosol concentrations there will be an increase in number concentrations of cloud droplets formed. These more abundant yet smaller droplets will be more reflective, giving the cloud a higher albedo (Twomey, 1974). The second indirect effect, or cloud lifetime effect, proposed by Albrecht suggests that with higher aerosol concentration there will be smaller cloud droplets that will take longer to develop into precipitation size droplets. Therefore, the cloud will have a longer lifetime and therefore be able to reflect more solar radiation than clouds in regions with lower aerosol concentrations (Albrecht, 1989). Though these mechanisms are understood in theory, better quantification of these and other radiative processes that influence cloud cover and precipitation are needed to better understand how the global radiation budget is changing as aerosol composition changes.

The impacts of water soluble aerosols on clouds do not only affect the radiation budget, but also affect the Earth's hydrological cycle. Aerosols can affect the total evaporation from the oceans, total global precipitation and can alter the distribution, duration and amount of precipitation events. Multiple studies have shown that precipitation can be suppressed over areas with high anthropogenic aerosol emissions (Kucienska, 2009; Ramanathan et al., 2001; Rosenfeld, 1999). The latest Intergovernmental Panel on Climate Change Report suggests that the largest uncertainty in the predicted change in the global radiation budget due to anthropogenically induced climate change arises from the uncertainty of the impact from aerosols (IPCC, 2007). Global radiative direct forcing and the cloud albedo effect are estimated to have changed by -0.50 and -0.70 W m^{-2} respectively since 1750. The corresponding assigned uncertainties for the direct forcing contribution are $\pm 0.40 \text{ W m}^{-2}$ and between -1.1 and $+0.4 \text{ W m}^{-2}$ for the albedo effect. The uncertainty in both sign and magnitude of aerosol radiation forcing further motivates more research on gaining a better understanding of all aerosol properties.

Aerosol optical properties also influence visibility which can degrade as aerosol concentrations increase, particularly with water soluble and hygroscopic aerosols that can have high water content and thus large scattering cross sections. Visibility is particularly important in scenic areas such as the United States National Parks. One monitoring network, the Interagency Monitoring of Protected Visual Environments (IMPROVE) network, was initiated in 1985 to provide information to better mitigate impacts on visibility. With long term sampling sites in protected areas such as the National Parks, the IMPROVE network provides a useful history of long term aerosol measurements.

Another monitoring network that started in 1991 is the Clean Air Status and Trends Network (CASTNET) which also monitors air quality at sites away from urban sources but includes sites outside of National Parks. Though good long term measurements have already been gained from both monitoring networks, comparison studies show that there may be discrepancies between the data in each network that are due to artifacts in the filter samples (Lavery et al., 2009; Sickles and Shadwick, 2008).

1.1.2 Challenges of Aerosol Measurements and Instrumentation

The challenge of regulating and mitigating aerosols for each environmental or health concern requires a variety of instrumentation and aerosol sampling techniques to gain specific information about the aerosol properties. The abundance of aerosol emission sources, varying lifetimes and chemical reactivity make thorough characterization of aerosols difficult. However, understanding the nature of atmospheric aerosol particles is necessary before impacts on the issues mentioned previously can be well understood and mitigated effectively. Numerous offline, semi-continuous and real-time aerosol characterization techniques have been developed and each one has their own advantages and disadvantages.

Offline analyses such as particle collection by filters have been used extensively to collect reliable aerosol composition data, but suffer from poor time resolution. For example, the IMPROVE network generally collects 24 hour time resolved filter samples every third day and CASTNET only collects weekly filter samples. Samples collected offline have been analyzed by a variety of techniques including gas, liquid or ion

chromatography (GC, LC and IC, respectively) which can also be coupled to a mass spectrometer (MS). Other techniques can measure specific groups of species, such as measuring the organic carbon and elemental carbon (OC and EC) in the carbonaceous fraction of aerosol particles, have also been developed to analyze offline filter samples. In addition to limited time resolution, another complication to offline sample analysis is the potential for sampling artifacts, so the measured concentrations may not be entirely representative of actual ambient concentrations (Prather et al., 2008). As one example, filters are susceptible to underestimating ammonium and nitrate because of the high volatility of ammonium nitrate. If ammonium nitrate particles are initially captured onto a filter and the temperature increases, the particles will volatilize and become lost. Methods like putting an additional filter inline after the initial filter to capture the volatilized nitrate have been used, but complicate the sampling procedure (Seinfeld and Pandis, 2006).

To decrease the potential for sampling artifacts and increase temporal resolution, there has been a focus on developing real-time aerosol collection techniques (Sullivan, 2005). A series of different aerosol mass spectrometry (AMS) instrumentation has been developed for real-time continuous aerosol composition measurements for either single particle analysis or bulk aerosol measurements. Some major AMS instruments include the Aerodyne AMS and the ATOFMS (Jayne et al., 2000; Noble and Prather, 1996). The main principle of the AMS consists of vaporizing and ionizing collected aerosol particles, which can be performed by a variety of methods, and then analyzing with MS. Some common particle ionizing techniques include laser desorption with laser ionization and

thermal desorption with electron or chemical ionization (Hartonen et al., 2011). Depending on the particle's unique characteristics, these different techniques create a range of ionization efficiencies, ionized products and collection efficiencies. Analysis by MS can be performed using a time of flight (TOF) technique, which is the most common and enables the collection of high resolution and size resolved particle measurements (Drewnick et al., 2005). Quadrupoles or ion traps are also common methods used in the AMS. Despite major advances in increasing the time resolution of aerosol measurements, several limitations exist in these instruments that use MS. High instrument costs prevent widespread use. Analysis is often complex and can yield only semi-quantitative results. In addition, the AMS does not measure any refractory compounds and also is limited by the ionization efficiencies of each compound.

Though some semi-continuous measurements that have been developed more recently focus on the collection of water soluble particles, the methods to collect water soluble particles have been extensively used. In order to detect and analyze submicron particles, they must be enlarged to enable particle collection by methods such as impaction. Collection of aerosol particles by condensational growth in the presence of steam has been used since the late 19th century. Utilizing adiabatic expansion to create condensation, Aitken developed a chamber that grew particles in his "dust counter" instrument (Aitken, 1897). More recently a variety of techniques have been developed that all use condensation to grow particles that can be easily collected and analyzed by a variety of methods. The Steam Jet Aerosol Collector (SJAC) introduces steam into a chamber that uses turbulence to mix with the collected aerosol sample (Khlystov et al.,

1995; Slanina et al., 2001). After the particles are enlarged, they can be collected by impaction or in a cyclone to form a liquid sample. The liquid sample can then go on to a variety of analysis techniques, with a common method being IC. One notable system that has taken the use of steam generation to be able to collect a liquid sample is the particle into liquid sampler (PILS) which can be coupled to IC for aerosol composition measurements. For PILS-IC analysis, a separation of inorganic ions can be done in less than four minutes and soluble organic acids, such as oxalic acid require a separation time of 15-30 minutes (Orsini et al., 2003). Since the separation in ion chromatography is dependent on the charge of each compound being analyzed, only ionic compounds can be separated. However, the ionic nature of most common aerosol components facilitates the use of this separation technique for ambient aerosol samples. Another instrument utilizing the growth of particles with steam is the monitor for measuring aerosol and gases (MARGA). In this method, a cyclone is used to capture the particles after condensational growth which are then analyzed using IC (ten Brink et al., 2009; Trebs et al., 2004). Thus, sample analysis times are also limited by the separation times of the IC.

A new instrument, aerosol chip electrophoresis (ACE), was developed with the advantages of being able to perform rapid aerosol composition measurements, improved sensitivity to comparable methods, lower manufacturing cost and small size footprint. Currently ACE is designed to measure the compositional characteristics of water soluble $PM_{2.5}$ by quantifying the concentrations of sulfate, nitrite, nitrate, chloride and oxalate. A cyclone followed by a growth tube enables the collection of water soluble $PM_{2.5}$.

Using microchip capillary electrophoresis for sample analysis followed by conductivity detection allows for sample collection on the order of one minute with good sensitivity. In addition, this technique facilitates a small footprint and low manufacturing costs. These characteristics make the ACE ideal for field studies where geographical and spatial resolution of aerosol composition is desired.

1.2 ACE Instrument Theory

The ACE instrument consists of three main components: the growth tube, microchip within a specially designed box, and the conductivity detector. The ACE system with all components except the sample vacuum pump, denuders and cyclone is shown in Figure 1.1. The ambient air sample first passes through a denuder to remove interfering acidic gases and a cyclone to remove all particles with an aerodynamic diameter greater than 2.5 μ m. The sample then enters the growth tube where the now enlarged particles can then be deposited onto the microchip. The aqueous aerosol sample is then injected from the sample reservoir into the separation channel of the microchip. After separation, the signal is detected by the conductivity detector. The details of each component are described in each section below.

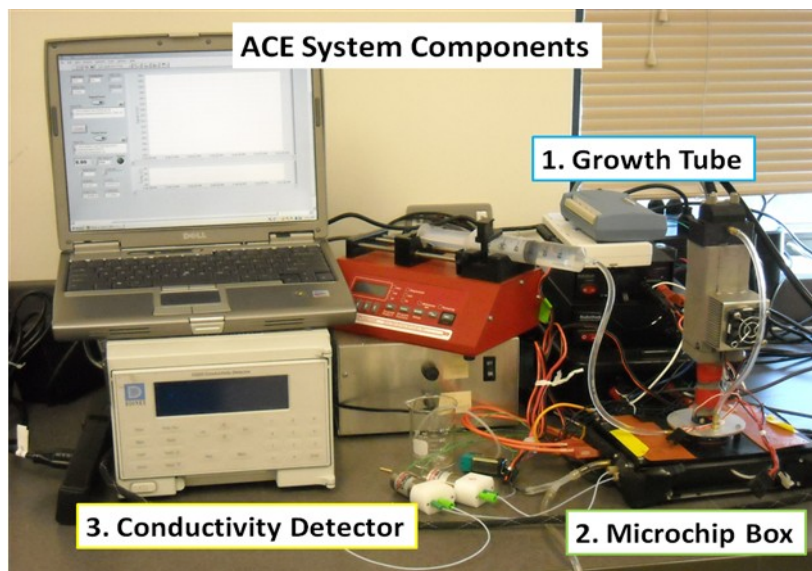


Figure 1.1: A photograph was taken showing the ACE system and the major components were labeled.

1.2.1 Particle Collection with a Growth Tube

Ambient particle collection is performed using a water condensation growth tube. The growth tube, developed at Aerosol Dynamics, Inc., was modeled after the growth tube in a laminar-flow water condensation particle counter (WCPC) (Hering and Stolzenburg, 2005). On the interior of the growth tube is a passively wetted wick of 9.2 mm inner diameter and 250 mm length which is composed of a porous hydrophilic plastic material. The wick is situated in a water reservoir that is automatically replenished with a syringe pump to keep it continuously saturated. This wetted wick creates saturation vapor pressure at the inner wall of the growth tube. The laminar sample flow is introduced into the top of the growth tube which is cooled. The second half of the growth tube is warmed, forming a steep temperature gradient. The temperature profile is depicted in Figure 1.2. This configuration creates supersaturated conditions inside the growth tube based on the difference in water vapor diffusivity and thermal diffusivity rates. The rate

of heat transfer through air, $0.215 \text{ cm}^2 \text{ s}^{-1}$, is slower than the rate that water vapor can travel through air, $0.265 \text{ cm}^2 \text{ s}^{-1}$. Since the water vapor can travel faster from the wall to the centerline, supersaturation forms within the warm region of the growth tube, reaching the highest level at the centerline. In other words, the introduction of the cooler sample air into the warmer second half of the growth tube allows for condensation to occur.

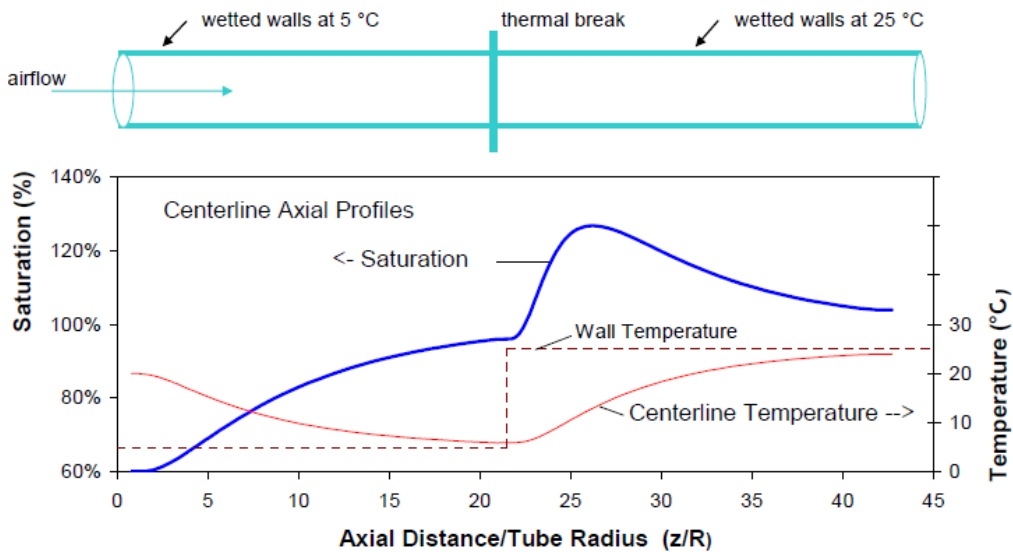


Figure 1.2: The typical temperature and saturation profiles formed in the growth tube are shown as a function of axial distance to tube radius (z/R). The wall temperature is also indicated, marking the thermal break in the controlled temperature of the growth tube (Hering et al., 2009).

In contrast to the traditional alcohol based particle counters, where the mass diffusivity of butanol is less than the thermal diffusivity of air, the temperature profile is reversed (Agarwal and Sem, 1980). In the alcohol based particle counters, the sample air is initially warmed and introduced to a cooler region where the butanol readily condenses onto the particles. In the water based growth tube used in the ACE instrument, particles grow by water condensation until a near monodisperse size distribution is achieved. The

condensational growth rate of the particles, $I_{(v)}$ by change in volume v , is described in Equation 1.1 where a constant density (ρ) is assumed (Seinfeld and Pandis, 2006). The term $f(Kn, \alpha)$ represents a correction due to both noncontinuum effects and imperfect surface accommodation, where Kn is the Knudsen number and α is the molecular accommodation coefficient. Condensational growth also depends on the diffusion coefficient of the species i in air (D_i) and the difference in the environmental vapor pressure and the equilibrium vapor pressure ($p_i - p_{eq,i}$). When the vapor pressure of the particles is not in equilibrium with the environmental vapor pressure, either condensational growth or evaporation will occur. In the supersaturation region of the growth tube, p_i is greater than $p_{eq,i}$, so condensational growth occurs.

$$I_{(v)} = \frac{dv}{dt} = \frac{2\pi^{\frac{2}{3}}(6v)^{\frac{1}{3}}D_iM_i}{\rho_pRT} f(Kn, \alpha)(p_i - p_{eq,i}) \quad (1.1)$$

When ignoring other factors that can contribute to particle formation, loss or growth, the change in the particle size distribution due to condensational growth can be represented by Equation 1.2 which is called the condensation equation (Seinfeld and Pandis, 2006). In the growth tube the final size of the grown aerosol is not only monodisperse, but fairly independent of the initial particle size. This phenomenon can be explained by the slowing diameter growth rate as particles become larger. Small particles will grow more rapidly, so as particles grow in size their growth rate slows which essentially traps all the particles to near the same size.

$$\frac{\delta n(v,t)}{\delta t} = - \frac{\delta}{\delta v} [I_v(v,t)n(v,t)] \quad (1.2)$$

Unlike a CCN counter that controls supersaturation at levels that would be seen in the atmosphere, the growth tube creates a very high supersaturation to activate as many

particles as possible. However, as particle diameter decreases, increased vapor pressure due to the Kelvin effect prevents water vapor from condensing onto the particle and condensational growth cannot be initiated. For a particle of a pure compound, Equation 1.3 shows that the saturation ratio, $S (p_A/p_A^\circ)$, increases with an increase in surface tension, σ , or molecular weight, M (Seinfeld and Pandis, 2006). S decreases with increases in the particle radius (R_p), density (ρ_l) and temperature (T). The universal gas constant is represented by R . This equation shows that a larger supersaturation is needed to grow smaller particles because particles with a smaller diameter have a larger surface

$$S = \frac{p_A}{p_A^\circ} = \exp\left(\frac{2\sigma M}{\rho_l R T R_p}\right) \quad (1.3)$$

vapor pressure (p_A). By using this concept, a critical diameter was approximated by finding the Kelvin diameter at a chosen supersaturation that would activate 50% of that particle size. Though this equation does not take into account particle chemistry, it was used to model the growth tube particle collection efficiency under different supersaturation conditions and find a first approximation of the critical diameter. When considering the experimental conditions that were comparable to ACE conditions in future testing, the critical diameter for the growth tube with a temperature difference of 34°C and a flow rate of 0.7 L min⁻¹ was determined experimentally to be less than 7 nm (Hering et al., 2009).

When interfacing the growth tube to the collection reservoir some physical constraints had to be considered to ensure efficient particle collection, including taking into account the complications that arise from particle collection into a liquid reservoir. The rate of sample flow and size of the droplet as it exits the growth tube need to create the ideal

momentum for the particle in order to ensure impaction but not create an unstable air/water interface. The Stokes number in Equation 1.4, which is essentially the ratio between the particle stop distance and distance of the path of the flow before impaction, determines the impaction efficiency (Seinfeld and Pandis, 2006). The Stokes number is controlled by the particle diameter (D_p), particle density (ρ_p), slip correction factor (C_c), flow velocity (μ_0), and length of flow path (L). The Weber number in Equation 1.5 describes the stability of the air/liquid interface by comparing the kinetic energy of the sample flow (Q) to the surface tension (σ) of the liquid surface. The density of air (ρ_{air}) and jet diameter (D_{jet}) are also needed for this calculation. In order to experimentally

$$St = \frac{D_p^2 \rho_p C_c \mu_0}{18 \mu L} \quad (1.4)$$

$$We = \frac{16 \rho_{air} Q^2}{\pi^2 D_{jet}^3 \sigma} \quad (1.5)$$

determine the ideal operating conditions for the growth tube, a range of flows and jet diameters were tested while aiming for an ideal Stokes number of 0.22 and Weber number of less than 1.5 (Hering et al., 2009). Equations 1.6 and 1.7 show how the Stokes and Weber numbers can be used to determine the ideal flow velocity (Q) and jet diameter. The collection efficiency was found to increase when using the same jet diameter but decreasing the flow rate from 1 L min⁻¹ to 0.7 L min⁻¹.

$$Q = \frac{\pi We \rho_p \sigma D_{50}^2}{36 St \rho_{air} \eta} \quad (1.6)$$

$$D_{jet} = \left(\frac{We \sigma \rho_p^2 D_{50}^4}{81 St^2 \rho_{air} \eta_{air}^2} \right)^{\frac{1}{3}} \quad (1.7)$$

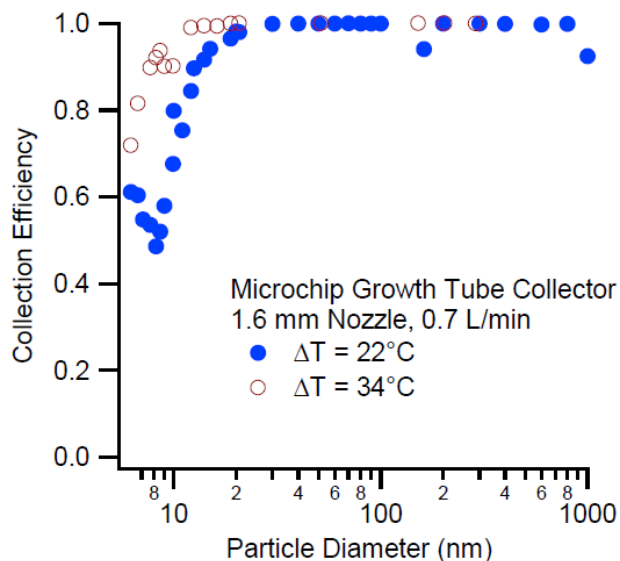


Figure 1.3: The collection efficiency was measured as a function of particle diameter with varying growth tube temperatures (Hering et al., 2009).

Additionally, changing the temperature difference (ΔT) was found to significantly impact collection efficiency, particularly for smaller particles, as shown in Figure 1.3. It was found that at a ΔT of 22°C in the growth tube and with a jet diameter of 1.6 mm and a flow of 0.7 L min^{-1} , the collection efficiency for was 99% for particles with diameter greater than 30 nm and 50% for particles with a diameter greater than 9 nm. When increasing ΔT to 34°C , collection efficiency was measured to be over 99% for 12 nm particles or larger and 50% for particles well below 10 nm in diameter (Hering et al., 2009; Noblitt et al., 2009a). By increasing the ΔT in the growth tube, the supersaturation increased which allowed for smaller particles to begin activating. This combination of flow rate and jet diameter allowed for the most efficient particle impaction and collection.

In the ACE system, the growth tube is placed directly above the microchip box as shown in Figure 1.4. Before the sample air enters the growth tube, gas phase nitric acid and

sulfur dioxide are removed with a denuder and particles larger than 2.5 μm in diameter are removed with a cyclone. After passing through the cooled region labeled the conditioner, the collected $\text{PM}_{2.5}$ sample enters the warm growth region where the particles are grown by the addition of condensed water vapor. The nozzle of the growth tube is placed directly over the sampler reservoir on the microchip. The grown particles are large enough for direct inertial impaction into the reservoir.

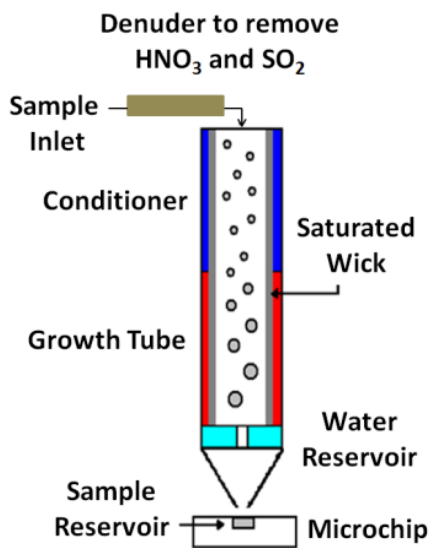


Figure 1.4: A schematic of the growth tube in the ACE system depicts the denuder that removes gases before the ambient sample enters the growth tube, the conditioner and growth region of the growth tube, and the microchip sample reservoir where the particles are impacted.

1.2.2 Separation Using Microchip Capillary Electrophoresis

The separation technique utilized in the aerosol chip electrophoresis (ACE) system, microchip capillary electrophoresis (MCE), has several advantages when compared to other separation techniques such as chromatography. One advantage of MCE is that it has a much smaller footprint than the comparable traditional CE or IC instruments. This is particularly useful for field work when the transport of instrumentation is needed or at

field sites where space is limited. Not only does a MCE instrument have a size advantage to comparable instruments, it is generally less expensive to manufacture than other continuous instruments such as PILS-IC or AMS. In a comprehensive aerosol field study, it would be possible to deploy multiple instruments over one region to gain improved spatial resolution. This spatial resolution would be desirable in locations with numerous pollution point sources such as a densely populated urban area where health effects would be a concern for the many residents living close to emission sources (Felhofer et al., 2010). Also, spatial trends of aerosol composition due to transport could be monitored by running multiple ACE instruments in one region.

In addition to having a much smaller size, MCE also has better separation efficiency and resolution of peaks compared to chromatographic techniques such as IC. By using high voltage to create a large electric field in the separation channel of the capillary electrophoresis (CE) separation, complete separations can be performed in under one minute. When sampling inorganic ions and organic acids, IC separation times can range from 4 to 30 minutes (Orsini et al., 2003). The separation speed in chromatography is limited by the amount of pressure able to be applied to the separation channel but in MCE is modified by the amount of voltage applied which can create a strong electric field. The electrically driven sample flow in CE can perform separations much faster than the pressure driven flow in chromatography methods. The force used in each separation technique to control sample flow also directly impacts sample peak resolution. The flow profile set up by the electroosmotic flow (EOF) enables better resolution of sample peaks. CE sample flow has an almost flat vertical profile due to the electric double layer that

essentially carries the solution through the channel. In contrast, methods like IC have a hyperbolic flow profile due to the pressure driven flow through the channel. The frictional forces on the sides of the channel cause the flow to slow down close to the channel walls. This flow profile causes band broadening, while the CE flow profile allows for the detection of sharper sample peaks.

The greater sensitivity and selectivity that CE can achieve when compared to methods like IC is a major advantage when measuring ambient aerosol samples that are generally low in sample mass. Finally, the smaller amounts of buffer needed compared to the eluent needed for IC separation make CE more ideal for field operation. In contrast to the IC that uses eluent on the order of 1 mL min^{-1} , the sample reservoir for ACE uses $21.5 \text{ }\mu\text{L}$ buffer and is replaced approximately every hour and the buffer reservoirs hold up to 1.5 mL and can be replaced every three days. The small sample volumes collected combined with smaller buffer volumes needed for the separation give CE the advantage of creating much less waste than other conventional chromatography systems. In contrast to other chromatographic separations, CE has the ability to modify the buffer to alter the migration times of individual species. This buffer can be altered to separate species specific to the collected sample.

For this study, the aerosol species chosen for analysis are commonly found in atmospheric aerosol. The inorganic anions chloride, sulfate, nitrate, and nitrite and organic oxalate are all separated by the ACE system. Using data from monitoring networks such as IMPROVE and CASTNET, aerosol composition measurements have shown that inorganic ions such as sulfate, nitrate and ammonium are highly variable

based on location within the United States (Hand, 2011). Notably, total $PM_{2.5}$ mass in eastern North America is comprised of one-fifth to one-half sulfate. In California, nitrate makes up over one-quarter of total $PM_{2.5}$ mass (McMurry et al., 2004). Oxalate, the only organic acid currently detected by the ACE system, is the most abundant dicarboxylic acid present in atmospheric aerosols (Mader et al., 2004; Rompp et al., 2006).

In the separation technique of microchip capillary electrophoresis (MCE), high voltage is applied to an ionic solution containing the collected aqueous sample which sets up an electric field in the separation channel. The components in solution can then be separated based on different migration times due to variations in charge and drag forces. The relative migration rate of each component (v) is determined by both the electrophoretic mobility (μ_e) and the electric field strength (E). The electric field strength is determined by the length of the channel and the voltage applied, which is held constant in the MCE system. Therefore, it is the electrophoretic mobility of each ionic component which is based on the charge and frictional forces of each component that determines v . In the MCE system, the background electrolyte (BGE) in the separation solution buffer also contributes to the absolute migration time of each component based on the EOF. The speed and direction of the EOF also contributes to the total mobility of each ionic component being separated. The electroosmotic mobility (μ_{eo}) is determined by the EOF. Both the μ_{eo} and μ_e influence the migration rate, as shown in Equation 1.8. (Skoog et al., 2007)

$$v = (\mu_e + \mu_{eo})E \quad (1.8)$$

The surface groups on the separation channel directly affect the EOF. The microchip in this application is made from poly(dimethylsiloxane) (PDMS). This creates a negatively charged surface due to the presence of silanol groups. The zwitterionic surfactant added to the custom developed buffer solution forms an electric double layer on the surface of the channels (Noblitt et al., 2009b). This allows the bulk solution in the separation channel to flow towards the anode when voltage is applied creating a reverse EOF. A reversed EOF could potentially decrease the resolution of the separation, but in this MCE application the separation is sufficiently fast that any decrease in resolution is negligible.

The microchip used in the ACE instrument was designed specifically for this application (Noblitt et al., 2009a). Voltage is supplied to the microchip from a high voltage power supply. The basic design of the microchip channels and reservoirs are shown in Figure 1.5. A high negative voltage is applied to two of the reservoirs, A and B, and the remaining two reservoirs are grounded, which creates an electric field and initiates the EOF in the separation channel. The EOF flows from D, the waste reservoir, to A, the sample reservoir. In normal operation, the solution flows from B to D due to the channel size and configuration. In order to inject a sample plug into the separation channel, the voltage of the buffer reservoir, B, is dropped to favor the flow from the sample reservoir, A, to the buffer waster reservoir. When a sample plug is injected it travels through the separation channel and passes the detection wires, labeled as E in Figure 1.5.



Figure 1.5: The basic design for buffer reservoirs and channels in a microchip is shown. (A) is the sample reservoir, (B) is the buffer reservoir, (C) is the buffer waste reservoir, (D) is the sample waste reservoir and (E) is the detection electrodes.

Figure 1.6 shows the microchip in the microchip box used in the ACE instrument. This shows the inside of the box that is directly under the growth tube, as labeled in the photograph of the entire instrument set up (Figure 1.1). The growth tube is attached to the lid of the microchip box which is sealed to keep the microchip at isobaric conditions. Additionally, heaters attached to both the top and bottom on the outside of the microchip box regulate the temperature of the microchip inside the box. The high voltage wires (red box), grounded wires (black box) and detection wires (yellow box) are labeled. The separation channels are highlighted in red with the detection wires highlighted in yellow.

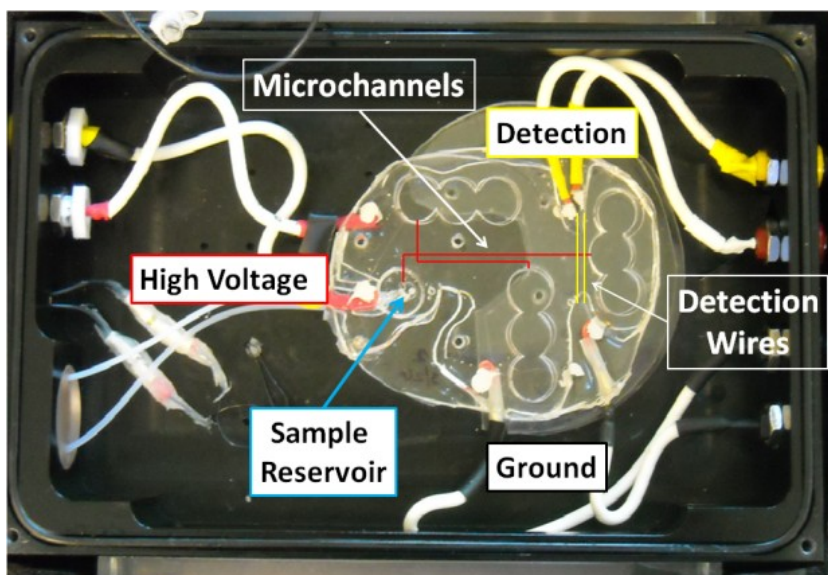


Figure 1.6: The ACE microchip as connected to wires leading to the high voltage supply and ground and the conductivity detector are shown in this photograph. The channels and detection wires are also highlighted.

The aerosol chip electrophoresis (ACE) instrument was the first instrument developed to measure the chemical composition of ambient aerosols using MCE. A specific buffer solution was created to achieve an efficient separation of chloride, sulfate, nitrate, nitrite and oxalate in collected samples (Noblitt et al., 2009b). Three different components were added to the buffer solution. Picolinic acid was added to control the pH at 4.7. This buffer component will also bind to oxalate, increasing its drag force and thus increasing the migration time. A zwitterionic surfactant, N-tetradecyl-N,N-dimethyl-3-ammonio-1-propanesulfonate (TDAPS), will form micelles around the aqueous nitrate ions and increase the migration time. Another compound, N-(2Hydroxyethyl)piperazine- N'-(4-butanesulfonic acid) (HEPBS), was added to bind to sulfate ions to also increase the migration time. The concentrations of each component were adjusted to provide the best resolution and separation of each analyte.

Also added to the buffer solution was 1,3-propanedisulfonate (PDS) which acted as an internal standard. The PDS was able to account for dilution due to deposition of condensed water in the sample reservoir and any differences that occur between injections. The amount and concentration of the collected sample will vary with time and can alter the ionic concentration in solution. This can affect the amount of sample injected, the time of separation and the detected signal. Similarly, sample dilution by condensation affects the volume of the sample over time. Though the change in sample volume is non-linear, changes in concentration should be proportional in both PDS and the sampled analytes so the internal standard will correct for the changes in volume.

1.2.3 Conductivity Detection Method

Traditionally, CE instrumentation has most commonly been paired with optical detection methods such as absorbance or laser induced fluorescence (LIF) (Gotz and Karst, 2007). LIF has the advantage of being sensitive enough for analysis of single molecules and is easily coupled to a CE instrument. However, this detection method is only effective for compounds that naturally fluoresce or can be modified to do so. Even for molecules that can fluoresce after being modified, the derivatization process to enable detection is typically time intensive and not practical for real-time measurements. The small inorganic ions that are of interest in aerosol particles are not fluorescent in nature and most do not absorb in the visible wavelength region, so another detection technique was needed. An electrochemical method, conductivity detection, has been previously used in other MCE applications (Guijt et al., 2004). Detection using conductivity has proven to

have the selectivity and sensitivity needed for the inorganic anions and organic compounds of interest in this work (Noblitt et al., 2009b).

Two different methods of conductivity detection, contact or contactless, were considered in order to determine which would provide the best compromise between maximizing sensitivity and minimizing BGE interference with the detection wires. In contact conductivity detection, the electrodes are placed in direct contact of the sample solution in the separation channel. In contactless detection, the electrodes are placed on either side of the separation channel. Both methods have been extensively used in MCE and each has advantages in certain applications (Uchiyama, 2004). In the ACE system, the initial issue was achieving high enough sensitivity for the low concentrations sampled, so contact conductivity was the method chosen. However, placing the electrodes directly into solution can create some difficulties as the electrode can interact with the BGE and sample. Over time, reaction with the BGE can cause electrode fouling and can eventually completely dissolve the electrode wire. Additionally, the electrodes can react with the water in solution at high voltages. This electrolysis reaction can create bubbles of hydrogen and oxygen at the electrodes and interfere with the separation. These issues were corrected for in the ACE system by using inert platinum or platinum and iridium blend electrode wires and by creating a bubble cell design at the detection cell. The platinum wires were inert and did not react with the BGE. The bubble cell did not significantly reduce sensitivity, but allowed for a lower electric field across the two detection wires which prevented electrolysis (Noblitt and Henry, 2008). By using contact conductivity detection, the maximum sensitivity could be achieved.

1.3 Previous Measurements with ACE

As a prototype field instrument, ACE has gone through a variety of changes since its initial development to improve operation for field measurements. In an initial study performed at Colorado State University in Fort Collins, Colorado, the ACE system was operated for over one day and was able to collect near continuous data alongside a PILS-IC for a comparison study in the summer of 2009. For this study, a previous microchip design and previous instrument set-up for ACE was used. Shown in Figure 1.7, the time line of sulfate and nitrate concentrations from both the PILS-IC and ACE instruments show very good agreement (Noblitt et al., 2009a). The average concentrations of sulfate measured were $0.48 \mu\text{g m}^{-3}$ by the ACE system and $0.39 \mu\text{g m}^{-3}$ by the PILS-IC, and $0.23 \mu\text{g m}^{-3}$ and $0.27 \mu\text{g m}^{-3}$ for nitrate by the ACE and PILS-IC, respectively. After averaging 3 injections for sulfate and 5 injections for nitrate, PILS-IC sulfate concentrations were found to be 19% lower than ACE measurements and PILS-IC nitrate concentrations were 18% higher for nitrate. The measurement discrepancies between instruments were determined to be reasonable considering that the concentrations measured by the PILS-IC were near the limit of detection.

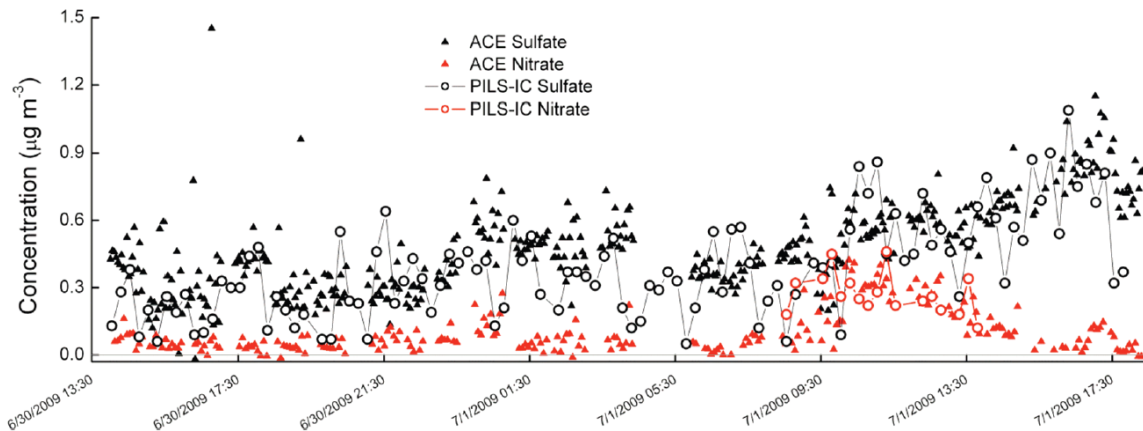


Figure 1.7: Sulfate (black) and nitrate concentrations (red) were measured by the ACE system (triangles) and compared with a PILS-IC (open circles). The sampling time resolution was 15 minutes for PILS-IC sulfate and nitrate, 5 minutes for ACE nitrate and 3 minutes for ACE sulfate.

In addition to showing that good comparison between the ACE and PILS-IC is possible, this field study showed that the ACE can achieve higher sensitivity compared to the PILS-IC. This was proven when low concentrations of nitrate were able to be detected by the ACE but the concentration was below the LOD of the PILS-IC. Nitrate was collected by ACE from when the sampling started until about 9:00 on July 1 when the concentration rose high enough to be captured by the PILS-IC. Even though some averaging was necessary to reduce data scatter, the ACE measurements were still better time resolved by a factor of three and five for nitrate and sulfate respectively.

Furthermore, ACE was able to detect low concentrations of oxalate which was not possible in the inorganic ion separation conditions of the PILS-IC.

Several factors prevented the system from running continuously in this field study that can be attributed to the instrument design at the time of the study. Noticeable gaps in ACE data were the result of temporary instrument failure that required manual system

adjustments before normal operation was restored. The lack of temperature control of the microchip box allowed for the formation of condensation when the room temperature decreased. Condensation inside the box can be damaging to the electronics of the system and prevent proper separation or detection of the aerosol sample. The microchip design used in the experiment limited the use of the BGE to three hours before enough ion depletion occurred and replacement was needed, which would prevent long term sampling in field studies. These sampling issues were later addressed and corrected to enable long term sampling.

Following this initial field study, the ACE system has been deployed on several field projects both in and outside of Fort Collins in a variety of environments ranging from pristine to heavily polluted. To date, field studies have been conducted in Fort Collins, CO in Summer 2009 and Spring 2011, Mariposa, California in March 2010, Rocky Mountain National Park in Colorado in September 2010, Bakersfield, California in January 2011 and Sugar Pine, California in Spring 2011. For the work presented here, measurements collected at two of those sites, Rocky Mountain National Park and Fort Collins in the spring of 2011, are analyzed in detail. In addition to field studies, laboratory testing with generated aerosol samples has also been able to provide insight into the capabilities and weaknesses of the ACE instrument. The work presented here represents only a portion of the collaborative efforts in the development of the ACE instrument, but considers a variety of tests the ACE instrument has completed which have lead to several modifications to improve ACE. Improvements to ACE will continue to be made to extend system operation by increasing automation, improve sensitivity and time

resolution of measurements, and maintain low manufacturing costs and small size to enable the collection of quality aerosol composition measurements in field studies.

CHAPTER 2. MATERIALS, METHODS AND CALCULATIONS

2.1 Project Overview

The ACE system was tested in multiple field studies and in laboratory experiments to determine instrument performance and viability for field measurements. The system was composed of a denuder to remove acidic gases and a cyclone for the collection of PM_{2.5}. The particle collection component consisted of a condensation growth tube. The aqueous aerosol sample is separated by microchip capillary electrophoresis in a temperature and pressure controlled environment and followed by conductivity detection. Two field studies were performed in Rocky Mountain National Park in Colorado (RMNP) in September 2010 and in Fort Collins, Colorado (FC) in June 2011 which compared measurements by the ACE and a PILS-IC. For additional comparison, filter samples were also collected in RMNP. Laboratory experiments measuring generated ammonium sulfate particles by ACE were also conducted in April 2011.

2.2 Materials

The microchips were fabricated in-house using Sylgard 184 elastomer base and curing agent, purchased from Dow Corning (Midland, MI), in custom molds. The material polydimethylsiloxane (PDMS) was chosen because it is easy to use, inexpensive and transparent to allow for visual inspection after the completion of the microchip. It is also relatively simple to modify the microchip by redesigning the molds. Gold-plated

tungsten wire, platinum/iridium, and platinum microwires were purchased from GoodFellow Corp. or California Wire Company.

The anion separation buffer contained N-tetradecyl-N,N-dimethyl-3-ammonio-1-propanesulfonate (TDAPS) purchased from Fluka, and picolinic acid (PA) and N-(2-hydroxyethyl)piperazine-N'-(4-butanesulfonic acid) (HEPBS) purchased from Sigma-Aldrich. The internal standard used was 1,3-propanedisulfonate (PDS), also purchased from Sigma-Aldrich. For PILS separation, a solution of sodium carbonate and sodium bicarbonate with the internal standard lithium bromide (LiBr) was used for the anion eluent. For the generated aerosol experiments, an ammonium sulfate solution was used. All standards and solutions were made using deionized water (18 M Ω -cm).

2.3 Methods

2.3.1 Microchip Fabrication

The microchips were fabricated from three layers of PDMS created from a custom designed mold. The designs on the three molds were created to imprint the reservoir outlines, guide post outlines and sample channels and wire channels on the appropriate layer. After placing the microwires in their channels, each microchip layer was sealed using plasma oxidation. Three pieces of 25 μ m diameter platinum wire were placed in the buffer, buffer waste, and sample waste reservoirs. Two detection electrodes of 20 μ m diameter platinum, platinum and iridium blend or gold plated tungsten wire were placed directly across the separation channel in a bubble cell. The bubble cell expanded the width of the separation channel at the detection zone four times the width of the

separation channel to improve detection (Noblitt and Henry, 2008). To each microwire, a larger insulated copper wire was permanently attached using silver paint and a layer of PDMS to allow for easier connection to the power supply and detection leads, as shown in Figure 2.1.

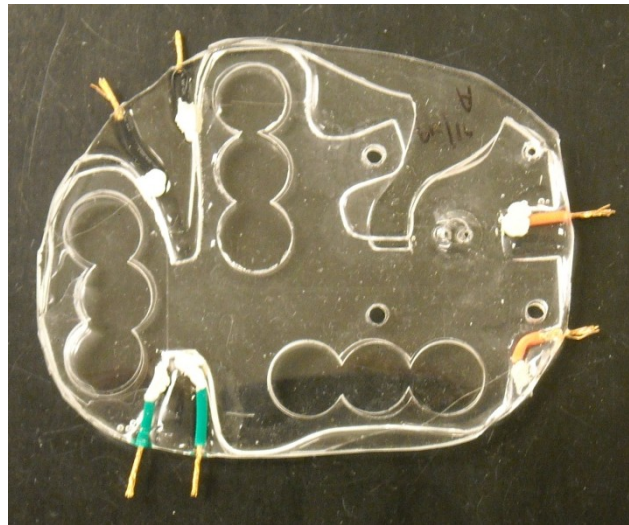


Figure 2.1: This photograph shows the most recent microchip design as used in both RMNP and FC field studies.

The microchip reservoirs and guide post holes were created with biopsy punches. The buffer, buffer waste, and sample waste reservoirs were created with three 12 mm diameter punches each. Each of the three holes slightly overlapped to create a large reservoir. The sample reservoir punch was 4 mm in diameter. Below the sample reservoir, the adjacent layer was punched with two 1 or 1.5 mm holes and the bottom layer was punched with an 8 mm hole. This allowed for the insertion of two pieces of 1/16 inch outer diameter tubing for flushing the sample reservoir. After inserting the tubing, additional PDMS was placed in the 8 mm hole around the tubing to secure it. To allow proper alignment of the microchip in the microchip box, four 3 mm holes were punched in the chip for guide posts. The top layer of the microchip design as well as the

channels and wires, as described above, is shown in Figure 2.2. The dimensions of the completed microchip were 6 mm in height, and about 6 cm in width and 8 cm in length. The separation channel was 5.2 cm long. Further information on microchip fabrication can be found in (Noblitt and Henry, 2008) and (Liu et al., 2000).

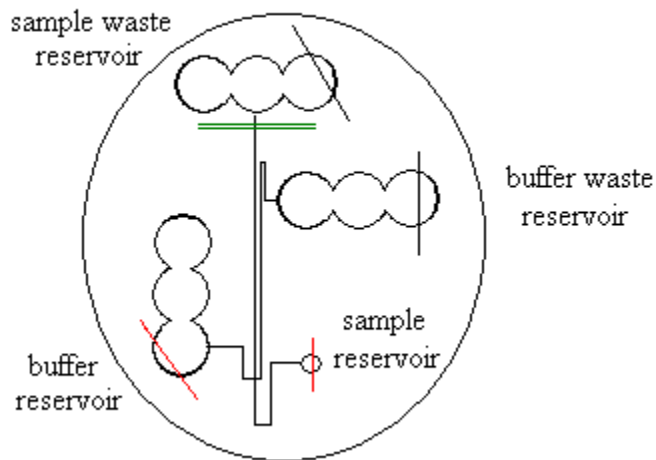


Figure 2.2: The microchip design is shown with labeled reservoirs and all sample channels. The microwires are color coded with red being at a high negative voltage, black at ground and green indicates the detection wires.

Controlled by thermoelectric devices and a custom made LabView control program, the growth tube temperature varied between 1-5°C and 30-35°C to maintain a specific temperature differential. The wetted wick on the interior of the growth tube provided the water vapor needed for supersaturated conditions. The bottom of the wick was submerged in a water reservoir that was continuously replenished with a syringe pump filled with DI water. The flow of the syringe pump was calculated based on sampling temperatures and flow rate of the growth tube to keep the water reservoir filled.

For standard microchip operation, the sample reservoir and buffer reservoir were kept at -2200V while the sample waste and buffer waste reservoirs were kept at ground. For gated injection, the voltage of the buffer reservoir was changed to -676 V for 0.8 to 1.5 seconds depending on sampling conditions. The brief change in electric field allowed a plug of sample to be injected into the separation channel for analysis. The reservoir voltages were controlled by a custom made LabView program. Though variable depending on the pump used, about 21 μL buffer solution was injected into the sample reservoir with the flushing tubing. During each sample flushing, the buffer solution was injected and removed three times. This ensured that no sample carry over from the previous analysis would contaminate the following sample analysis.

The temperature of the microchip box was controlled by the same LabView program to be heated between 27-30°C to prevent condensation on the microchip box interior but also minimize sample evaporation from elevated temperatures. The temperature of the microchip box depended on the warm temperature of the growth tube, ensuring the box temperature was always greater. However, the box temperature could not be too high or sample evaporation becomes an issue. In addition to being temperature controlled, the closed microchip box also creates isobaric conditions. The conditions in the microchip box eliminate the possibility of hydrodynamic flow influences on the electrophoresis separation. The microchip box is especially important for keeping the microchip at a constant temperature and pressure in field studies where the sampling environments can change significantly over short time periods.

2.3.2 *Standard ACE Operation*

The sample flow rate through the growth tube was measured at the sampling entry point into the growth tube with a Gillian Gilibrator. Flow rates into the growth tube were checked periodically throughout each sampling period for a total of three measurements at RMNP and five measurements at FC. For the best representation of the flow rate during the actual data collection, the flow measurements taken before, during and after when usable data were collected were weighted and averaged assuming any measured changes in flow rate were linear over time. The average flow rate was 0.80 L min^{-1} for RMNP and 0.72 L min^{-1} for FC. The flow rate along with the total sampling time for each data point were used to calculate the total volume of sampled air used in ambient concentration calculations. An initial test was performed to ensure no leaks existed in the microchip box by additionally measuring the flow into and out of the microchip box. The percent change in the flow into the box was less than 1% compared to the flow out of the box, which indicated a minimal amount of leaking. No corrections to total sample volume collected were deemed necessary.

Calibration standards for sulfate, nitrate, oxalate, and chloride were prepared gravimetrically to minimize error in calculated concentration. To each calibration standard, $20 \mu\text{M}$ of internal standard was also added. The peak areas were integrated using a Gaussian fit. To form the calibration curve, the peak area ratio of each analyte to the internal standard was calculated and plotted on the y axis. On the x axis, the ratio of concentration of analyte to internal standard was plotted. The calibration curve used a least squares fit and the intercept was forced through zero.

2.3.3 Instrumentation for Generated Aerosol Experiments

For the generated aerosol particle tests, ammonium sulfate particles were generated with an atomizer from a 1 g L^{-1} ammonium sulfate solution into a sample tank as shown in the instrument set up in Figure 2.3. The generated ammonium sulfate particles were size selected in a differential mobility analyzer (DMA) and the resulting sample was split and led to a condensation particle counter (CPC) and the ACE system. Various concentrations were achieved by changing the particle diameter using the DMA and by changing the dilution flow going into the tank.

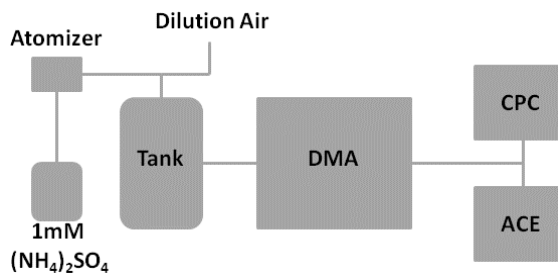


Figure 2.3: The instrument set up of generated aerosol shown was used to make comparison measurements between the ACE and CPC.

2.3.4 PILS-IC Operation

A PILS-IC was used in each field study to compare measurements with the ACE. Only the anion separation of the IC was needed for comparison tests. The PILS instrument was developed to collect water soluble aerosols. By using a steam injector and mixing chamber, aerosols can be mixed with the steam and undergo condensational growth. At the end of the chamber an impaction plate collects the enlarged particles which then runs into a sampling line that is directed towards two different ICs for either anionic or cationic separations (Orsini et al., 2003; Weber et al., 2001). The separations in ion

chromatography are pressure driven and elution times are based on the size and charge of each compound being analyzed.

Calibration curves were also created for each field study. The calibration curves used for both RMNP and FC data were compared with two other calibration curves created in the past two years for validation. Five calibration standards were used to create the nitrate calibration curve with concentrations ranging from 1 to 25.8 μN . Each standard was injected manually with a micropipette into the microchip sample reservoir after the previous sample was removed with the flushing pumps. This injection and flushing cycle was performed a total of three times to best mimic how the collected ambient aerosol sample is treated during ACE field operation. For the sulfate calibration curve, five standards with concentrations ranging from 2 to 50 μN were used. Each calibration curve for both nitrate and sulfate had a least squares linear regression value or correlation coefficient (R^2) of at least 0.998. Blank DI water samples were also measured periodically throughout the sampling periods. The nitrate calibration curves were fit using the calculated y intercept. However, the low sulfate concentrations measured in the field necessitated fitting the sulfate calibration curve through zero to prevent the calculation of negative concentrations.

Katherine B. (Beem) Benedict operated the PILS-IC at RMNP and Amy P. Sullivan assisted with operation in FC as well as the formation of the calibration curves. The sample inlet was fitted with a $\text{PM}_{2.5}$ cyclone as well as two denuders to remove both acidic and basic gases according to standard PILS operating procedures. For ACE

comparison, only the removal of the acidic gases that could interfere with the anion separation was necessary. In both field studies, the sample flow rate of the PILS was 15 L min⁻¹. The separation was performed using an eluent of 1.8 mM Na₂CO₃/1.7 mM NaHCO₃ at a liquid sample flow rate of 1 mL min⁻¹. A Dionex AS14A column was used with a Dionex ASRS ULTRA II suppressor. A sample loop was continuously filled and a sample was injected and analyzed every 17 minutes.

2.4 Calculations

2.4.1 Ambient Aerosol Calculation for ACE

The aqueous concentrations of the chemical species of interest measured by ACE must be converted to their corresponding ambient concentration. During sample collection, consecutive injections are continuously added to the sample reservoir between sample flushing. Therefore, the ambient concentrations are determined by the change in the aqueous concentration of the analyte, *i*, ($C_{i, \text{aq}}$, $\mu\text{mol L}^{-1}$) over the collection time (*t*, seconds), which is represented in the Equation 2.1 as $\frac{dC_{i, \text{aq}}}{dt}$. To find the concentration at any particular time, the difference in concentration from the previous injection is calculated. In order to convert the aqueous analyte concentration into ambient aerosol concentration ($C_{i, \text{aer}}$, $\mu\text{g m}^{-3}$), the sampling rate (Q_{samp} , L min⁻¹) and volume of the sample (V_{liq} , mL) must be measured. The molecular weight of the analyte (M_i , g mol⁻¹) along with a unit conversion factor are also needed for the conversion to $C_{i, \text{aer}}$.

$$\frac{dC_{i, \text{aq}}}{dt} = \frac{50C_{i, \text{aer}}Q_{\text{samp}}}{3M_iV_{\text{liq}}} \quad 2.1$$

In order to account for any variation between injections, such as dilution in the sample reservoir due to condensed water deposition and changes in the injection volume as the conductivity of the sample varies with the amount of collected sample or after ion depletion, an internal standard is used. The calibration curve is formed using both the concentration (C) and peak area (P) ratio of the internal standard to species *i*. Assuming that any changes in the internal standard peak area will be proportional to the changes in the peak area of the analyte with each injection, the ratios to calculate concentration will remove any injection to injection biases. The calculation for $C_{i,aq}$ is shown using the peak area ratio, concentration of internal standard (C_{IS} , $\mu\text{mol L}^{-1}$) and the slope from the calibration curve (F).

$$C_{i,aq} = \frac{C_{IS}P_i}{FP_{IS}} \quad 2.2$$

The above equations for $C_{i,aq}$ do not take into account the ion depletion effect that arises from standard MCE operating conditions. Though the main sample flow controlled by EOF is much stronger than the electrical forces on each individual analyte, the ions from the buffer solution and sample can migrate due to their charge. Since the compounds of interest are anionic in nature, they will tend to migrate towards the waste reservoir, which is acting as the anode. Similarly, cationic compounds in the buffer solution can slowly migrate towards the cathode (Pu et al., 2004). The ion depletion is enhanced over time, so buffer solution must be replaced before the change in composition significantly alters the separation conditions. This ion depletion effect can be quantified by the last term in Equation 2.3 shown below. Since this term is dependent upon $C_{i,aq}$ and the mobility of each analyte (μ_i , $\text{cm}^2 \text{s}^{-1} \text{V}^{-1}$), the magnitude of ion depletion of the analyte ions over time varies by each compound and thus any changes in ion concentrations of the analytes are

nonlinear. The ion depletion is also affected by the mobility of the EOF (μ_{EOF} , $\text{cm}^2 \text{ s V}^{-1}$), the electric field (E , V cm^{-1}) and cross-sectional area of the separation channel (A , m^2). To accurately calculate $C_{i,\text{aer}}$, the experimental conditions were altered so that this ion depletion term was negligible and Equation 2.1 could be used to calculate ambient concentration.

$$\frac{dC_{i,\text{aq}}}{dt} = \frac{50C_{i,\text{aer}}Q_{\text{samp}}}{3M_iV_{\text{liq}}} - \frac{10^7 C_{i,\text{aq}} E(\mu_i + \mu_{\text{EOF}})A}{V_{\text{liq}}} \quad 2.3$$

2.4.2 Sulfate Calculation Using the CPC

Using the size as selected by the DMA and the number concentration measured by the CPC, the sulfate concentration of the generated ammonium sulfate (AS) aerosol was calculated. The particles generated had a mean diameter of 30, 50 or 100 nm. The concentration of sulfate in the generated aerosol, $[\text{SO}_4^{2-}]_{\text{aer}}$ is calculated in Equation 2.4 by assuming the particle is spherical with uniform composition and density (ρ_{AS}). The particle volume ($\frac{4}{3}\pi r^3$) was calculated and combined with the particle number as measured by the CPC (N_{AS}), the molecular weight (MW) of both sulfate and AS and the density of AS (ρ_{AS}) to find $[\text{SO}_4^{2-}]$.

$$[\text{SO}_4^{2-}]_{\text{aer}} = \frac{4}{3}\pi r^3 N_{\text{AS}} \rho_{\text{AS}} \frac{\text{MW}_{\text{SO}_4^{2-}}}{\text{MW}_{\text{AS}}} 10^{-9} \quad 2.4$$

The calculated sulfate concentration was then corrected for influence by doubly and triply charged particles. A 10:1 sheath flow, temperature of 298.2 K, and pressure of 837 mb were used in the calculation. Since the mean particle size was known and the size distribution was unknown, a size distribution was created to estimate the number of

multiply charge particles with known mean particle diameter (D_{pg}) and assumed standard deviation (σ_g) of 1.8. For each particle size that was generated, the mobility (Z_p) was determined by Equation 2.5. The variables include the charge of the particle (n), elementary unit of charge (e), slip correction factor (C_c), viscosity (η), and particle diameter (D_p). Since Z_p is proportional to n and inversely proportional to D_p , the diameters of the doubly and triply charged particles that would be captured by the DMA could be calculated. Using the known fraction of each particle size that is charged by the DMA and the sulfate concentration of each particle size collected, the total sulfate concentration could be calculated.

$$Z_p = \frac{neC_c}{3\pi\eta D_p} \quad 2.5$$

2.4.3 PILS-IC Calculation

Ambient $PM_{2.5}$ aerosol concentrations were also measured by a PILS-IC. The calculation presented in Orsini et al, 2003 to determine ambient concentrations of common inorganic anions is shown in Equation 2.6. Oxalate was not detected by the PILS-IC. $[C_g]$, the ambient aerosol concentration, was found by measuring $[C_L]$, the concentration of the species of interest in the aqueous sample. For the conversion from aqueous concentration to ambient concentration, the flow of the transport liquid spiked with the internal standard entering the impactor (q_{in}), the ratio of the internal standard concentration entering the impactor over the concentration exiting the impactor (R) and the volumetric flow rate of the sample air (Q_a) are used. The internal standard is added to account for sample dilution from the steam collection. The calibration curve was used to convert integrated peak areas as measured by IC to $[C_L]$.

$$[C_g] = [C_L] q_{in} \frac{R}{Q_a} \quad 2.6$$

2.4.4 Statistical Calculations

The percent difference calculation, Equation 2.7, was used to determine the difference in ambient concentration measurements between two different methods. The values from two methods, x_1 and x_2 , are compared.

$$\text{Percent Difference} = \frac{|x_1 - x_2|}{\frac{x_1 + x_2}{2}} * 100 \quad 2.7$$

In contrast, the 95% confidence interval was calculated as a measurement of the variability between consecutive ACE measurements when averaged to match the time resolution of the PILS-IC measurements. The student's t value (t) at the 95% confidence level, standard deviation (s) of the average value and total number of samples (n) are used. The relative 95% confidence interval was also calculated by dividing by the average value and multiplying by 100. Additionally, the absolute value of the 95% confidence interval was taken.

$$\text{95\% confidence interval} = \pm \frac{ts}{\sqrt{n}} \quad 2.8$$

The limit of detection was calculated for each experiment for the ACE measurements. The student's t value for the 95% confidence interval was used with the standard deviation of measured blanks (s_b), the total number of samples (N_1) and the number of blank samples (N_b). To find the blank signal for the ACE system, a LabView program was used to view and segment one second pieces of baseline that were collected during each sampling period. The standard deviation of the one second segments of the baseline was calculated and each section was averaged to gain a total blank signal for each field

study. The number of samples (N_1) represented the average amount of raw ACE measurements averaged into one 17 minute averaged data point.

$$LOD = \pm ts_b \sqrt{\frac{N_1 + N_b}{N_1 N_b}} \quad 2.9$$

As a measure of instrument precision, the uncertainty in the final ambient aerosol concentration arises from the various components of the ACE system. These components include the sample flow rate (q), sample volume (v), internal standard concentration (is) and the chemical measurements (c) and must all be taken into account for a total uncertainty calculation. Representing uncertainty with the absolute value of the relative 95% confidence interval (RCI), the total was found using Equation 2.10.

$$Total\ uncertainty = \sqrt{(RCI_q)^2 + (RCI_v)^2 + (RCI_{is})^2 + (RCI_c)^2} \quad 2.10$$

A constant value was calculated for the sample flow rate, Q_{smp} , sample volume, V_{liq} , and internal standard concentration, C_{IS} . The uncertainty from each component is expressed as the relative 95% confidence interval. The deviations in Q_{smp} were previously calculated at approximately 3% (Noblitt et al., 2009a) when using older brass valves. This is a generous approximation for the samples taken in the field study in FC and for the generated aerosol tests because more precise Swagelock valves replaced the older brass valves used at RMNP which would have improved uncertainty in Q_{smp} . The uncertainty in V_{liq} was calculated by measuring the volume dispensed by the flushing pumps gravimetrically. With 19 replicate measurements, the volume dispensed was 16.40 μ L with a standard deviation of 0.28 μ L, giving an uncertainty of 0.8%. Deviations in the internal standard concentration would arise from the uncertainty in the pipettes and balances used to prepare the internal standard solutions. To calculate the uncertainty in

the concentration, replicate measurements of the internal standard concentration in the calibration standards were used (n=12) and found to be 3%.

The uncertainty in the chemical measurement was by far the most important contribution to the total uncertainty. The uncertainty in the chemical measurement was found by calculating the relative 95% confidence interval for each 17 minute averaged ACE concentration. On average, each averaged concentration used 12 ACE measurements for both sulfate and nitrate in both studies. This represented the uncertainty specific to the amount of averaging performed in this study.

2.5 Quality Assurance and Quality Control

If a significant issue with instrument performance that prevented sample collection and analysis was observed, the data were rejected. Issues included improper instrument set up or malfunctioning instrumental components. Some collection issues had clear indications in the collected conductivity signal. For example, random and sharp spikes in the signal were observed and attributed to a poor connection in the detection wires of the microchip at the end of the sampling period in RMNP. When there is a break in the connection, the conductivity detection will increase almost instantly to the maximum signal, causing sharp spikes in the signal. This was evident as the microchip performance deteriorated towards the end of the sampling period; thus, data collected after September 21 were rejected.

With low concentrations measured for both sulfate and nitrate, data averaging was needed to improve the signal to noise ratio and gain better confidence in the results presented. Prior to peak analysis for the RMNP data, the electropherograms for every three injections were averaged, reducing the time resolution of the ACE system from one minute and 15 seconds to three minutes and 45 seconds. To verify that ensemble averaging improved peak resolution, the noise for both the original electropherograms and the averaged electropherograms was calculated. This was done by taking a ten second section of the data file when no peaks were detected and calculating the standard deviation of the signal. A large number of sections were averaged over the entire sampling period to get the best representation of the average noise. The average noise values as calculated using both the original and averaged electropherograms in RMNP are shown in Table 2.2.

Table 2.2: The average noise as calculated by averaging the standard deviation of the baseline signal (mV) is shown for the two data files collected over the sampling period. The number of baseline sections used to calculate the average standard deviation is shown in parenthesis.

	20110917 ROMO	20110919 ROMO
Original electropherograms	0.134 (50)	0.405 (36)
Averaged electropherograms	0.019 (30)	0.350 (30)

Additional averaging of the calculated ambient aerosol concentration was also done following the peak analysis which further reduced the time resolution. For the data collected in Fort Collins, no ensemble averaging of the electropherograms was performed. With more fluctuations in the peak migration times compared with the measurements in RMNP, ensemble averaging was avoided to prevent any peak shape distortion, which is possible if peaks of different migration times are averaged. After

determining ambient aerosol concentrations, the ACE data from both RMNP and FC were averaged in 17 minute intervals to match the PILS-IC measurements. In addition to allowing direct comparison between these measurements, this amount of averaging helped reduce data scatter while still maintaining good time resolution.

To compare ensemble averaging in the FC data, a section with a spike in high nitrate concentration between 17:26 on June 17 until 12:33 on June 18, 2011 was examined. The average nitrate concentration as measured by PILS-IC during this sampling time was $0.47 \mu\text{g m}^{-3}$. The concentration of nitrate with just boxcar averaging after calculating the ambient concentration was found to be $0.41 \mu\text{g m}^{-3}$. Similar to how the RMNP data were averaged, an initial averaging of three electropherograms was performed followed by boxcar averaging of the calculated nitrate concentrations to match the time resolution of the PILS-IC was performed. The average nitrate concentration from this method was $0.36 \mu\text{g m}^{-3}$, which is much lower than the calculated PILS-IC value. In this sampling campaign, this suggests that electropherogram averaging could distort the peak shape and justifies why electropherogram averaging was not used.

CHAPTER 3. RESULTS

3.1 Instrumental Conditions

The ACE system was deployed in three major field studies in Rocky Mountain National Park (RMNP); Bakersfield, CA and in Fort Collins, CO (FC). Instrumental malfunctions in Bakersfield, CA prevented the collection of any usable data; that campaign will not be further discussed here. The ACE system was deployed in RMNP during a larger field campaign that also measured gas phase species concentration, composition of precipitation and particle composition. Most notably, 24 hour URG filter samples and PILS-IC measurements were collected concurrently and compared to the ACE measurements. The sampling period occurred between September 16 and September 21, 2010 and resulted in just over four full days of continuous data. Over the five day sampling period, the buffer solution was replaced twice, on September 17 around 11:00 and on September 19 around 18:00. In the second field campaign conducted in FC, the ACE system made measurements between June 17 and June 24 in 2011 alongside a PILS-IC. In both studies, only nitrate and sulfate were detected and concentrations of chloride, nitrite and oxalate were well below the limit of detection and not observed during either sampling period.

The instrumental conditions differed between the two field campaigns. During the field study at RMNP, the growth tube temperatures were kept at 2°C at the cold end and 28°C

at the warm end for a temperature difference of 26°C. The microchip in the box was kept at 29°C. The injection length was 2.3 seconds and occurred every 75 seconds with 48 injections performed between each flushing cycle. During the sampling at FC, the growth tube temperatures were set to 1°C and 35°C. However, the growth tube struggled to keep the temperature at 1°C and was seen to rise as high as 6°C during the sampling. This would have given a temperature difference of between 29 and 34°C. The microchip box temperature was altered between 37 and 38.5°C depending on how much condensation was forming. Due to differences in ACE microchip performance during the field study at FC, the injection time was reduced to 1.2 seconds to prevent peak fronting. Additionally, the total number of injections performed before sample reservoir flushing was increased to 96 injections to allow more aerosol mass to be collected since low concentrations of both sulfate and nitrate were measured. The length of each sample analysis remained at 75 seconds. In each case, the sample reservoir was flushed by pulling the solution out with solenoid pumps, and replaced with clean buffer solution three times in succession to ensure complete removal of the previous sample. The sample flow rate was near 0.7 L min⁻¹. For comparison, previous successful measurements performed in Fort Collins used 1 L min⁻¹ sample flow rate, growth tube temperatures of 2 to 26 °C or 1 to 28 °C with the microchip box at room temperature (Noblitt et al., 2009a).

For data comparison, the 17 minute time resolved PILS data were used along with 24 hour time resolved URG filter data for additional verification. Thus, for comparison statistics, it was necessary for the ACE data to be averaged to match the PILS data, and

both ACE and PILS data to be averaged to compare to the URG filter pack data. In addition to normal data quality control procedures as described in the methods section, some data had to be discarded due to inadequate operational conditions because of improper instrument setup or instrument failure which were specific to each field study. A better understanding of these issues and solutions to solve any operational problems are crucial to be able to run the ACE system for extended sampling periods. A more descriptive analysis of the instrument failures and possible improvements will be presented in the discussion section below.

3.2 ACE Comparison Data

The ACE measurements for sulfate and nitrate concentration are compared with PILS-IC measurements collected in both RMNP (Figure 3.1) and FC (Figure 3.2). Sulfate and nitrate concentrations from RMNP are presented from September 17, 2010 at 11:40 am to September 21, 2010 at 7:52 am. Measurements from FC presented are from June 17, 2011 at 4:43 pm to June 24, 2011 at 7:26 am. Nitrate and sulfate concentrations in both periods were extremely low, with values typically below $0.5 \mu\text{g m}^{-3}$, making accurate quantification difficult. The time series of concentrations show reasonably good agreement for both sulfate and nitrate in RMNP, but much more scatter in ACE measurements from data collected in FC. The noise was too high after June 21 in the FC data set to detect nitrate peaks, but sulfate was still able to be quantified.

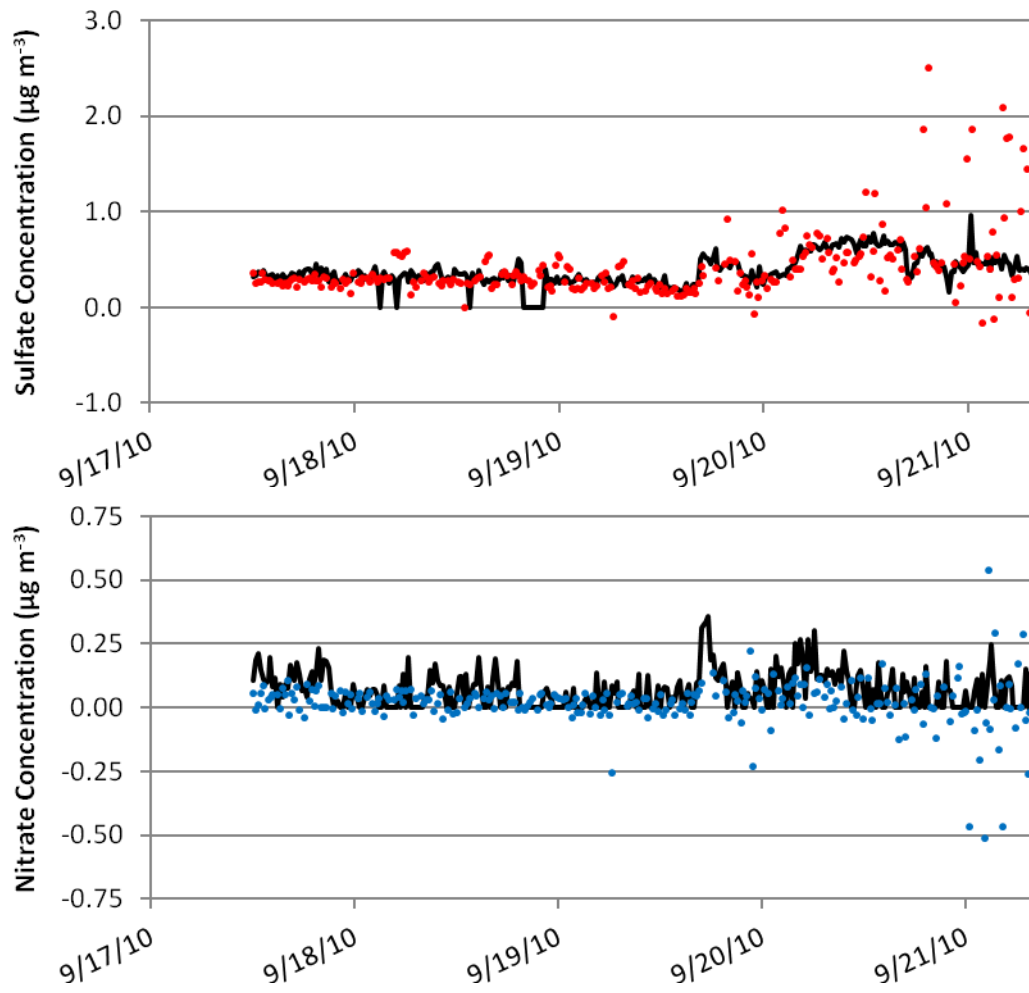


Figure 3.1: The concentrations of sulfate and nitrate measured in RMNP from September 17-September 21, 2010 using both the PLS-IC (black line) and the ACE (sulfate in red and nitrate in blue).

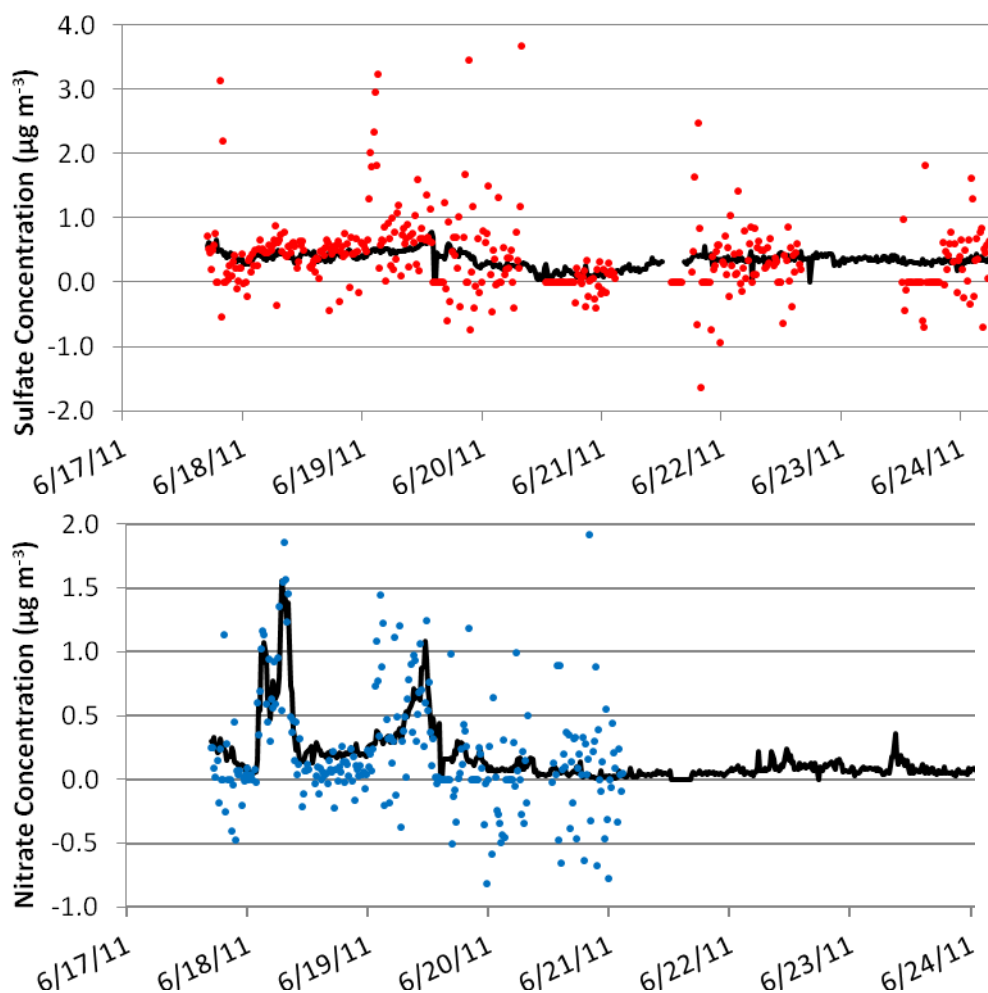


Figure 3.2: The concentrations of sulfate and nitrate measured in Fort Collins from June 17 to June 24 in 2011 using both the PILS-IC (black line) and the ACE (sulfate in red and nitrate in blue)

The sulfate and nitrate measurements collected in RMNP and FC were directly compared and plotted against a 1:1 line as shown in Figure 3.3. The differences between the two field studies are readily observed in these plots. In both RMNP and FC, the sulfate from both ACE and PILS-IC agreed well, but in FC the ACE measurements of sulfate had significantly more scatter. For nitrate, the concentrations at RMNP were too low to provide an easily observed comparison correlation, so the plot showing only RMNP

nitrate values was expanded and displayed in Figure 3.4. For the measurements taken at FC, there were high amounts of data scatter for both sulfate and nitrate but there was some agreement between PILS and ACE concentrations.

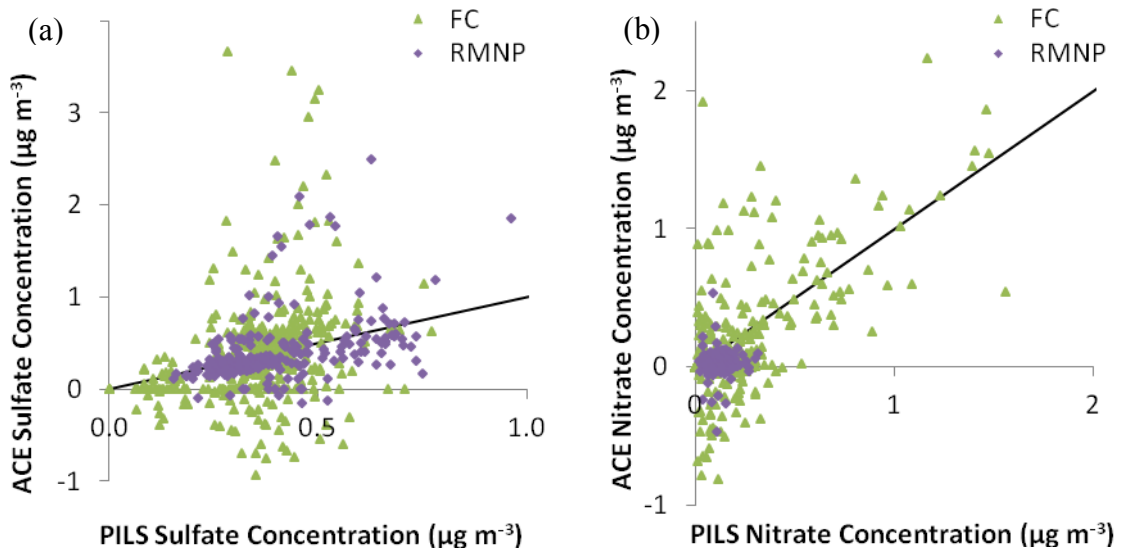


Figure 3.3: The measurements from PILS-IC are compared directly with measurements by ACE for sulfate (a) and nitrate (b). A 1:1 line is plotted as the solid black line.

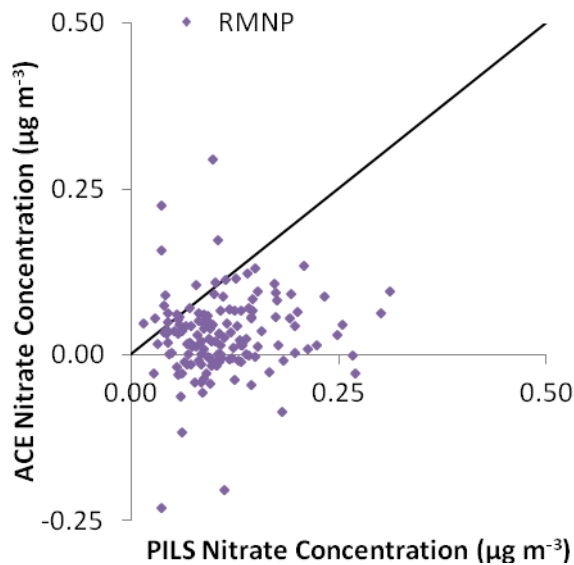


Figure 3.4: The measurements from PILS-IC are compared directly with measurements by ACE for nitrate collected in RMNP with a 1:1 line plotted in solid black.

To summarize both sulfate and nitrate concentrations in RMNP and FC, the average concentration over the entire sampling period for each site is displayed in Table 3.1 as measured by both the ACE and PILS-IC. As a measure of the variability or data scatter in the averaged ACE concentrations, the 95% confidence interval (CI) was calculated for each 17-minute averaged ACE concentration. The average of these 95% confidence intervals is displayed in Table 3.1. The percent difference between the average PILS concentration and the average ACE concentration for each field study is shown (overall percent difference). Additionally, to get a sense of how the individual measurements varied over the sampling period, the percent difference between each PILS measurement and its corresponding averaged ACE measurement (individual percent difference) were calculated and all values were averaged and displayed below.

Table 3.1: Average concentration and comparison statistics for sulfate and nitrate concentrations measured in RMNP and FC.

	RMNP		FC	
	Sulfate	Nitrate	Sulfate	Nitrate
Average PILS-IC Concentration ($\mu\text{g m}^{-3}$)	0.39	0.11	0.35	0.17
Average ACE Concentration ($\mu\text{g m}^{-3}$)	0.38	0.02	0.39	0.22
ACE 95% Relative Confidence Interval	50.1%	689%	2481%	-54.6%
Overall Percent Difference	1.8%	136%	-11.5%	-23.8%
Individual Percent Difference	10.3%	72.5%	498%	217%

In addition to comparing the ACE measurements with the PILS-IC, three days of URG filter data were also collected in RMNP that could be compared with ACE. In Table 3.2 below, the 24 hour resolved URG filter concentrations for sulfate and nitrate are listed with the 24 hour averaged ACE and PILS concentrations. Additionally, the percent difference between the ACE concentrations and the URG filter sample concentrations

and between the ACE concentrations and PILS concentrations for both sulfate and nitrate at RMNP were also calculated.

Table 3.2: Averaged daily concentrations as measured by the ACE, PILS, and URG systems for the only three full days of ACE data collected during the sampling campaign. In parenthesis are the calculated values of percent difference between the averaged daily concentrations as measured by the ACE system and PILS or URG measurements.

Date	Compound	ACE	PILS	URG
9-18	Sulfate	0.322	0.309 (4.4%)	0.244 (28%)
9-19		0.275	0.310 (-12%)	0.181 (41%)
9-20		0.580	0.541 (7.1%)	0.420 (32%)
9-18	Nitrate	0.045	0.089 (-65%)	0.042 (8.2%)
9-19		0.066	0.111 (-50%)	0.043 (65%)
9-20		0.098	0.132 (-29%)	0.050 (38%)

3.3 Generated Aerosol Experiment

For instrument validation tests, ammonium sulfate particles were generated, size selected by a differential mobility analyzer (DMA) and measured by both the ACE instrument and a condensation particle counter (CPC). Various concentrations and particle sizes were generated to enable the analysis of a range of atmospherically relevant conditions.

Particles with midpoint diameters of 30, 50 and 100 nm were generated in concentrations ranging from below the LOD to almost $25 \mu\text{g m}^{-3}$ as measured by the ACE instrument.

The growth tube flow rate remained near 0.7 L min^{-1} for the entire analysis. The temperature differential was controlled to 30°C at a minimum, ranging from $1\text{-}5^\circ\text{C}$ at the cold end and $35\text{-}36^\circ\text{C}$ at the warm end. The microchip box temperature was kept between 36 and 37°C , always at least one degree warmer than the temperature of the warm end of the growth tube. The microchip injection time was adjusted to either 0.8 or

1.5 seconds, according to the microchip box temperature. At higher box temperatures, the peaks would tend to broaden so a shorter sample injection time was preferred. The analysis time ranged between 60 and 90 seconds.

Six different samples as measured by both the ACE and CPC are shown in Table 3.3. The 95% confidence interval was calculated for the average concentration for each sampling period. Since the concentration remained at steady state during each sample period, the calculated 95% confidence interval represents the ACE measurement variability. Each injection was analyzed in 60 seconds and approximately 60 injections were performed for each sample. Large discrepancies motivated a closer look into the 30 nm and 100 nm particle diameter samples, which will be performed in the future. Only the samples using 50 nm diameter particles were plotted in Figure 3.5 showing the direct comparison between sulfate concentrations as measured by ACE and the CPC. The vertical error bars represent the 95% confidence interval of the average sulfate concentration as measured by the ACE instrument. Horizontal error bars for the CPC-derived sulfate concentration are plotted but are not visible due to the small value of the calculated 95% confidence interval of these data. Overall, the measured concentrations agreed very well between ACE and the concentrations determined from the CPC particle count and the selected particle size.

Table 3.3: The sulfate concentrations measured by ACE and CPC are listed with the relative 95% confidence interval in the parenthesis.

Particle Diameter (nm)	ACE Conc. ($\mu\text{g m}^{-3}$)	CPC ($\mu\text{g m}^{-3}$)
50	0.55 (15.20%)	0.55 (0.13%)
50	0.94 (32.31%)	0.90 (0.19%)
50	1.09 (23.82%)	1.57 (0.35%)
50	1.14 (18.03%)	1.12 (0.14%)
30	0.02 (290.76%)	0.30 (0.98%)
100	24.71 (24.93%)	12.95 (0.10%)

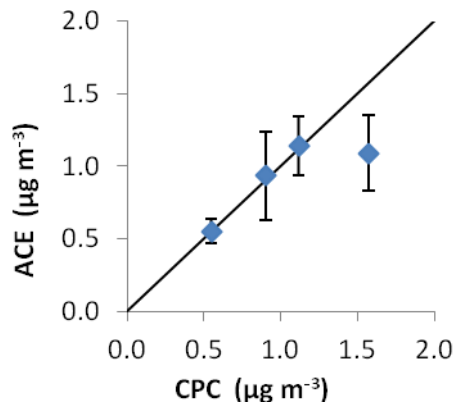


Figure 3.5: The sulfate concentration as measured by the ACE instrument are compared to the CPC for 50 nm diameter particles. Error in ACE concentration is represented by 95% confidence interval. The error in the CPC-derived concentration is not observable in this scale.

For the 30 nm particle diameter, the CPC-determined concentration was about an order of magnitude higher than the concentration measured by ACE, which was below the LOD.

For the 100 nm diameter particle sample, the measured concentration by ACE was twice as large as the concentration measured by the CPC at 24.71 and 12.95 $\mu\text{g m}^{-3}$,

respectively. Both of these measured concentrations were high, so it is possible that the sulfate concentration may have overloaded the ACE system. Though the generated particle concentration was at steady state, the concentration measured by ACE was not constant over the sampling period. The initial ACE concentration measured was

7.7 $\mu\text{g m}^{-3}$ sulfate, with concentrations as high as 51 $\mu\text{g m}^{-3}$ sulfate measured during the sampling period. While this suggests sulfate concentrations that are too high for the ACE to measure, further tests need to be performed on low and high sulfate concentrations to determine the true limits of the ACE instrument. Another consideration was a high particle number concentration of 13,200 cm^{-3} for this sample. At the same flow rate, but a lower temperature differential of 22 °C, the growth tube has been previously tested and shown to be able to efficiently collect particles at number concentrations up to 20,000 cm^{-3} . The higher temperature differential used in the generated aerosol experiment would not act to lower this concentration limitation, suggesting that the particle concentration measured in the experiment was within any growth tube concentration limitations. Finally, the uncertainties in the multiplet correction in the generated aerosol concentration calculation were considered. Since doublets and triplets have larger particle sizes and are expected to comprise a larger fraction in the 100 nm sample compared to the 30 and 50 nm samples, there could be a larger difference in sulfate concentration when adding the multiplet contribution. This might be contributing to the underestimation of the sulfate concentration by the CPC with respect to the ACE concentration. Unfortunately, multiplet concentrations were not experimentally quantified in the generated aerosol experiments.

CHAPTER 4. INSTRUMENT AND METHOD VALIDATION

4.1 Statistical Analysis of ACE Data

4.1.1 Instrumental Detection Limits

The limit of detection (LOD) was calculated for the ACE data using the calculation in the methods section and determined for both RMNP and FC. The LOD in RMNP was $0.137 \mu\text{g m}^{-3}$ for both nitrate and sulfate. The LODs in FC were higher than in RMNP, with nitrate and sulfate at 0.226 and $0.227 \mu\text{g m}^{-3}$, respectively. ACE LOD values provide an indication of the system noise in each case. Higher noise in the system would give a higher standard deviation in the signal of the blank sample. Since each sampling period involved large numbers of samples, the blank standard deviation had the most impact on the overall LOD. The higher LOD values calculated for the study in FC indicated the presence of more noise, which can also be observed in the time series of nitrate and sulfate concentrations displayed in Figure 3.2. Even though the LOD was calculated, all ACE values were retained for the purpose of determining concentration averages. If all values below the LOD were removed or changed to zero, including the negative values that were calculated, the averaged ambient aerosol concentration would be overestimated.

Table 4.1: The calculated ambient aerosol LODs for nitrate and sulfate in ACE are shown as measured in both RMNP and FC.

Sampling Location	LOD ($\mu\text{g m}^{-3}$)	
	Nitrate	Sulfate
RMNP	0.137	0.137
FC	0.226	0.227

The calculation for the LOD is directly related to the noise, which represents the measurement limitations of the instrument during field operation as seen in the values presented in Table 4.1. In a previous study, detection limits again were calculated based on a measured signal to noise ratio. The LODs were calculated to be 86 and 140 $\text{ng m}^{-3} \text{min}^{-1}$ for online samples of sulfate and nitrate, respectively, collected using a 1 L min^{-1} sample flow and a 30 μL sample volume (Noblitt et al., 2009a). Additionally, system blanks were collected during a different ambient aerosol analysis giving LODs for chloride and sulfate of 198 and 270 $\text{ng m}^{-3} \text{min}^{-1}$ (Noblitt, 2011). The LODs were calculated using a three injection averaging and signals for nitrate and oxalate were not detected. The PILS-IC LODs measured in a previous field study with 15 minute time resolved measurements for nitrate and sulfate were 90 ng m^{-3} and 60 ng m^{-3} , respectively (Lee et al., 2008).

4.1.2 Data Averaging Analysis

Boxcar averaging was used to average groups of consecutive ambient aerosol concentrations. The data were averaged primarily to reduce data scatter. The fluctuations in the peak areas for the internal standard and the analytes translated into enhanced fluctuations in the ambient aerosol component calculations. By averaging varying numbers of consecutive samples ranging from two consecutive points up to the entire data set from one day, which was almost 1800 points, the effects of averaging were

investigated. Additionally, averaging was necessary to be able to directly compare ACE data with PILS-IC measurements because of the difference in analysis times. ACE data were averaged to match both the 17 minute time resolution of the PILS-IC and the daily average of the URG filter measurements as available.

As expected, data averaging acted to smooth out features of the concentration time series in the ACE measurements. Using an example that had the highest fluctuations in concentration, the nitrate concentration measured in Fort Collins is shown in Figure 4.1 with varying degrees of averaging. Starting with the 17 minute averaged ACE data used in the PILS-IC comparison shown above in Figure 3.2, the data points were averaged an additional two, five and ten times. The least amount of averaging, represented by the green line, shows the most data scatter but also best matches some of the PILS-IC features at the highest concentrations observed on June 17. By averaging an additional ten times, shown in the blue line, the scattering is significantly reduced, but the trends in the nitrate concentration are smoothed out when compared to the PILS-IC measurements. This indicates the importance of averaging to reach an ideal compromise between reducing data scatter while keeping the highest time resolution possible.

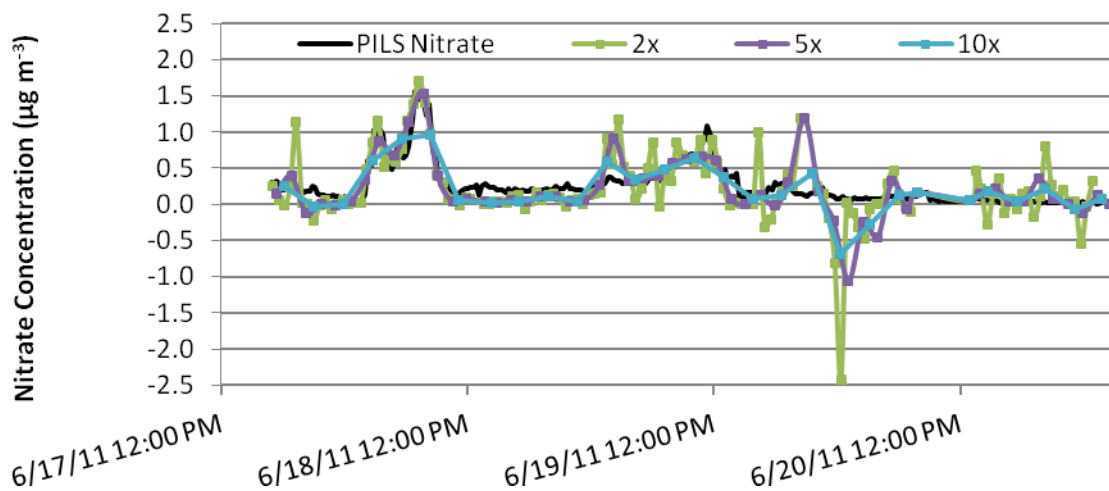


Figure 4.1: Nitrate measurements from PILS-IC (black line) were compared with measurements from ACE averaged an additional two, five and ten times the original 17 minute averaged data set used in Figure 3.2 (green, purple and blue squares and lines, respectively).

4.1.3 Variation in Measured Concentrations

Additional comparison between the PILS and ACE data on a higher time resolution was performed by looking at confidence intervals and relative standard deviations (RSD). The averaged relative 95% confidence interval (RCI) was calculated for all collected ACE measurements as shown in Table 4.2. First, the 95% confidence interval was calculated for each 17 minute averaged ACE data point and then divided by the averaged concentration for that time interval. However, to eliminate negative values arising from measured negative concentrations, the absolute value of each relative confidence interval was taken. In this way, the magnitude of the variability of consecutive ACE measurements could be retained by removing any negative values that would have acted to reduce the total magnitude of the RCI when averaged with positive values. The absolute values of each calculated relative confidence interval were averaged which gave an indication of measurement variability throughout each field study. Since each 17

minute time resolved PILS-IC data point was used in the analysis with no additional averaging, a different statistical approach was used to further investigate the collected measurements. The RSD was calculated for the measurements from each sampling point, which represented the natural variability in the ambient aerosol concentrations over the length of the sampling period.

Table 4.2: The averaged relative 95% confidence intervals (RCI) calculated for each 17 minute averaged ACE data point and the relative standard deviation (RSD) for the sulfate and nitrate concentrations as measured by the PILS-IC is shown for each field campaign.

	RMNP		Fort Collins	
	Sulfate	Nitrate	Sulfate	Nitrate
ACE RCI	55%	1190%	3080%	2690%
PILS-IC RSD	0.388±0.383	0.113±0.544	0.35±0.34	0.174±1.29

Since ACE data were averaged to match the 17 minute time resolution of the PILS, the RCI was calculated to gain a sense of how variable the data were within each 17 minute averaged point. Over most time periods during the sampling, the gradual increasing and decreasing concentrations as shown by the PILS-IC time series in Figures 3.1 and 3.2 suggest that concentration does not change rapidly. A gradual increasing or decreasing concentration implies that consecutive ACE measurements should not show much variation between consecutive injections. However, the large RCI values of over 1000% in three cases illustrate significant variation between the consecutive measured ACE concentrations within each averaged data point. This variation is also apparent from the amount of scatter seen in the ACE concentrations in Figures 3.1 and 3.2, particularly in the FC field study.

The large variations in the 17 minute averaged ACE data points could also suggest that the ambient concentrations are changing rapidly in a 17 minute time period. To further investigate this possibility, two 8 hour subsets of the nitrate concentration data measured on June, 18, 2011 in Fort Collins were analyzed. Between 2:00 and 10:00, nitrate concentrations spiked to high levels and quickly returned to low concentrations. For contrast, a stagnant period of low concentration between 15:00 and 23:00 was also considered. During the initial high concentration period, the RCI was found to be 260% and the second stagnant period of nitrate concentrations gave an absolute RCI value of 1060%. It is likely that for the stagnant period of low concentration, the concentrations near the LOD were harder to detect and contributed to more uncertainty in the measurements and therefore more scatter than when the concentration changed rapidly in the initial period. Additionally, the uncertainty in the calculated ambient aerosol concentration increases for lower concentrations (Noblitt, 2011). The average nitrate concentration during the initial high concentration period was $0.85 \mu\text{g m}^{-3}$ and the concentration during the stagnant period was $0.07 \mu\text{g m}^{-3}$, suggesting that values with low concentrations could play a significant role in the amount of data scatter in the ACE measurements. This is not surprising given the large uncertainty in concentrations below the system LOD.

In contrast to variation in the ACE measurements, the RSD in the PILS-IC data sets were calculated to express the magnitude of variation in concentration throughout the field campaigns. The moderate values for the relative standard deviation (RSD) as displayed in Table 4.2 suggest that concentration did change significantly during each sampling

campaign, particularly for nitrate during the Fort Collins study. The high RSD in nitrate can be explained by the peaks of nitrate that reached concentrations of $1.5 \mu\text{g m}^{-3}$ on June 18 and 19, 2011. In comparison, the concentration did not change much during the study at RMNP for either sulfate or nitrate.

4.1.4 ACE Calibration

A calibration curve for the ACE system was created for both studies at RMNP and FC. Six standards were created for the RMNP study and four standards were created for the FC study. The concentrations for each standard used and the R^2 of each calibration curve are shown in Table 4.3. With all R^2 values over 0.9938, a good linear regression is seen in each calibration curve for both field studies. Although different numbers of standards were used for each field study, the concentration range remained similar as did the R^2 values.

Table 4.3: The concentration of each standard (μM) for the sulfate and nitrate calibration curves is listed along with the R^2 value.

	RMNP		FC	
	Sulfate	Nitrate	Sulfate	Nitrate
Standard 1	3.89	3.92	3.43	3.59
Standard 2	5.02	5.07	10.51	11.00
Standard 3	9.69	9.76	28.61	29.95
Standard 4	20.05	20.21	60.72	63.57
Standard 5	34.59	34.87	-	-
Standard 6	51.42	51.82	-	-
R^2 value	0.9938	0.9965	0.9984	0.9987

The calibration curves for sulfate and nitrate created for both the RMNP and FC field studies are shown in Figure 4.2. Each curve was fitted with a linear trendline with the intercept forced through zero. The linear regression equations for each calibration curve

are shown for comparison. There are differences in the equations between the RMNP and FC studies, which can impact the final concentration calculated. To investigate the impact of the linear regression equation on the ACE ambient aerosol concentration, the concentrations of sulfate and nitrate were calculated using the linear regression equation from the other field study. When using the FC equation in the RMNP study, nitrate values were 17% different and sulfate values were 5% different. The same differences were observed when using the RMNP calibration curve equation in the FC data. Future evaluation efforts should continue to consider variability over time and between chips in system response and calibration curves.

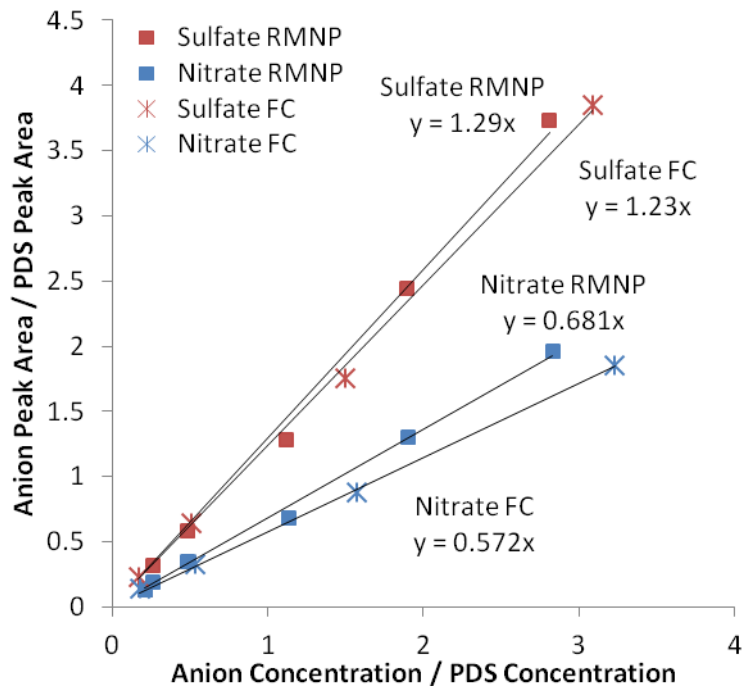


Figure 4.2: The calibration curves for sulfate and nitrate at both RMNP and FC field studies are shown with their linear regression equation.

4.2 Analysis of ACE Ambient Aerosol Calculation

The method of calculating the concentration of components in ambient aerosol from the ACE instrument differs from instruments such as the PILS. The aqueous sample in the PILS is collected continuously into a sample tubing loop and is injected every 17 minutes. For the ACE system, in comparison, sample is collected continuously but is also deposited continuously into the sample reservoir. The sample from the microchip reservoir is periodically injected, and represents the accumulated concentration over the entire time of sample collection. This method of collection requires that a differential calculation be used to determine the concentration at each injection.

Due to the differential method of calculation, there is the potential for obtaining negative values for the ambient concentrations, particularly when there is little change in peak area over time when low concentrations are being sampled. There are a variety of approaches to handle these negative concentrations which include giving the negative values a value of zero or using half of the LOD concentration. Each has significant impact when the concentrations are averaged. It was determined the most reasonable averaging method would be to include all negative values when finding average concentrations from the ACE instrument. This method was used to minimize bias introduced to the data when averaging these negative values.

4.3 Improvements in ACE

Numerous improvements, both major and minor, have been performed to the ACE instrument throughout this project. Only the major improvements will be discussed in

detail here. Testing the ACE instrument in the field allowed weaknesses of the instrument to be identified and improvements to be made. After the tests in Fort Collins performed in June and July 2009 were completed, the initial major improvements were to increase automation of the instrument to enable periods of longer sample collection without manual adjustments. To facilitate this, a new microchip design was created with smaller channels and larger buffer reservoirs (Noblitt, 2011). The smaller channels reduce ion depletion and the larger reservoirs hold more buffer to increase sampling time. This also allowed for longer sampling times between buffer replacements. Additionally, a smaller volume of flushing solution was added to the sample reservoir automatically with calibrated solenoid pumps which allowed for a higher concentration of the sample collected to be measured.

The field study in RMNP in September 2010 proved the effectiveness of the increased instrument automation by collecting measurements for five continuous days with minimal manual adjustments. The new microchip design with smaller channels and larger reservoirs was used with 15 μm gold-plated tungsten wire for the detection electrodes and 20 μm Pt wires for the reservoirs. Even though improvements were made to the automation of the ACE system, when compared to the tests performed in Fort Collins in the summer of 2009, new issues were seen in the ACE instrument. In the field study at RMNP, there was an increase in instrumental noise and much more data scatter in the ACE measurements for both sulfate and nitrate. This suggested more work was needed to reduce instrumental noise and improve the measurement signal to reduce data scatter.

Before testing in Bakersfield, CA in January 2010, the potential issue of a high sample flow rate that is not effectively collected in the microchip reservoir was addressed. To address this issue, ADI developed an attachment for the ACE instrument that was described as a “post-concentrator.” This additional component was placed on the underside of the microchip box lid directly underneath the growth tube. After passing through the growth tube, the sample flow then entered the post concentrator. The total sample flow rate was reduced while retaining the entire collected sample. Similar to an aerodynamic lens such as those present in an AMS, the now concentrated sample was then directed into the microchip reservoir but with a flow rate 1/5 of the original rate (Liu et al., 1995). Due to issues with instrument operation with the new post-concentrator, no data were collected in Bakersfield, so no concentration measurements using the post-concentrator are presented. However, the need for the post concentrator in the ACE instrument is questionable. During the preliminary generated aerosol tests, the ACE ambient aerosol concentrations were similar to the CPC derived concentrations suggesting there was no issue from the current sample flow rate of 0.7 L min^{-1} . Since the current flow rate did not affect the particle collection efficiency, the use of the post-concentrator may not be necessary. More tests using different aerosol concentrations, especially higher concentrations, are needed to further address this issue.

The ACE instrument for the generated aerosol test and comparison test in Fort Collins performed in May 2011 and June 2011, respectively, had few changes since the tests in RMNP. The same microchip design was used but with updated detection wires. It was seen that the gold coating on the gold-plated tungsten wires could crack and chip and the

exposed tungsten would dissolve, breaking the connection of the detection wires. First a solid platinum wire was used as it is a very inert metal and would not react with the BGE. The tensile strength of the platinum wire was lower than the gold-plated tungsten, and therefore created issues in the microchip fabrication and during transport and handling of the microchip. A platinum alloy was then chosen for improved tensile strength, but was tested to ensure there would be no significant increase in noise in the ACE system. The best compromise was found in the 80/20 platinum and iridium blend which replaced the gold-plate tungsten wires for the microchip's detection wires. Preliminary tests of this new wire showed the best combination of tensile strength and inertness for this application (Noblitt, 2011).

Instrumental noise still presents a significant problem when collecting ambient aerosol measurements on the ACE and many improvements have been performed in an attempt to reduce noise. Better wires and connections have been put in the microchip box to connect the power supply and detector to the microchip. The wires inside the microchip box were replaced with wires that were insulated from higher voltages to prevent arcing from the wires to the microchip box. The connection from the microchip box wire to the microchip wire was also replaced with a simple push pin style connector to relieve some torque that the terminal strip connections place on the microchip wires and to also provide better insulation. The detection wires are particularly susceptible to noise interference from the microchip box if not properly insulated, so additional measures are currently being taken to further reduce noise produced by the system.

To replace the Dionex CD-20, a new conductivity detector is being developed specifically for use with the ACE system. This new ACE component is being designed and constructed at the University of California at San Diego. The new detector is being designed with improved signal to noise when compared to the CD-20. Though additional testing is needed for online sampling, initial tests with an offline microchip have already shown it is capable of achieving higher measurement sensitivity (Noblitt, 2011). Additionally, the current detector design is much smaller than the CD-20 and will be able to reduce the overall footprint of the ACE system.

CHAPTER 5. DISCUSSION OF FIELD STUDY DATA

5.1 Description of Field Sites

Rocky Mountain National Park (RMNP) has low sulfate and nitrate concentrations in fine PM primarily due to its remote location. The prevailing wind direction is westerly from an area dominated by wilderness, but when the wind direction changes to easterly, particulate sulfate and nitrate can be transported from the urban corridor region of Colorado (Beem et al., 2010). Depending on the air transport patterns, there can be episodes of higher nitrate and sulfate in RMNP (Gebhart et al., 2011). Shown in the plots in Figure 5.1 are the concentrations of PM_{2.5} sulfate and nitrate measured in RMNP for 2010 (IMPROVE, 2010). The data shown here are from 24 hour filter samples that are collected every third day. Nitrate and sulfate concentrations vary throughout the year, but are generally lower than 1 $\mu\text{g m}^{-3}$ on a 24 hour average basis. In September, when the ACE data were also collected, the daily average sulfate concentration ranged from 0.2-0.6 $\mu\text{g m}^{-3}$ and nitrate concentrations ranged from 0-0.4 $\mu\text{g m}^{-3}$.

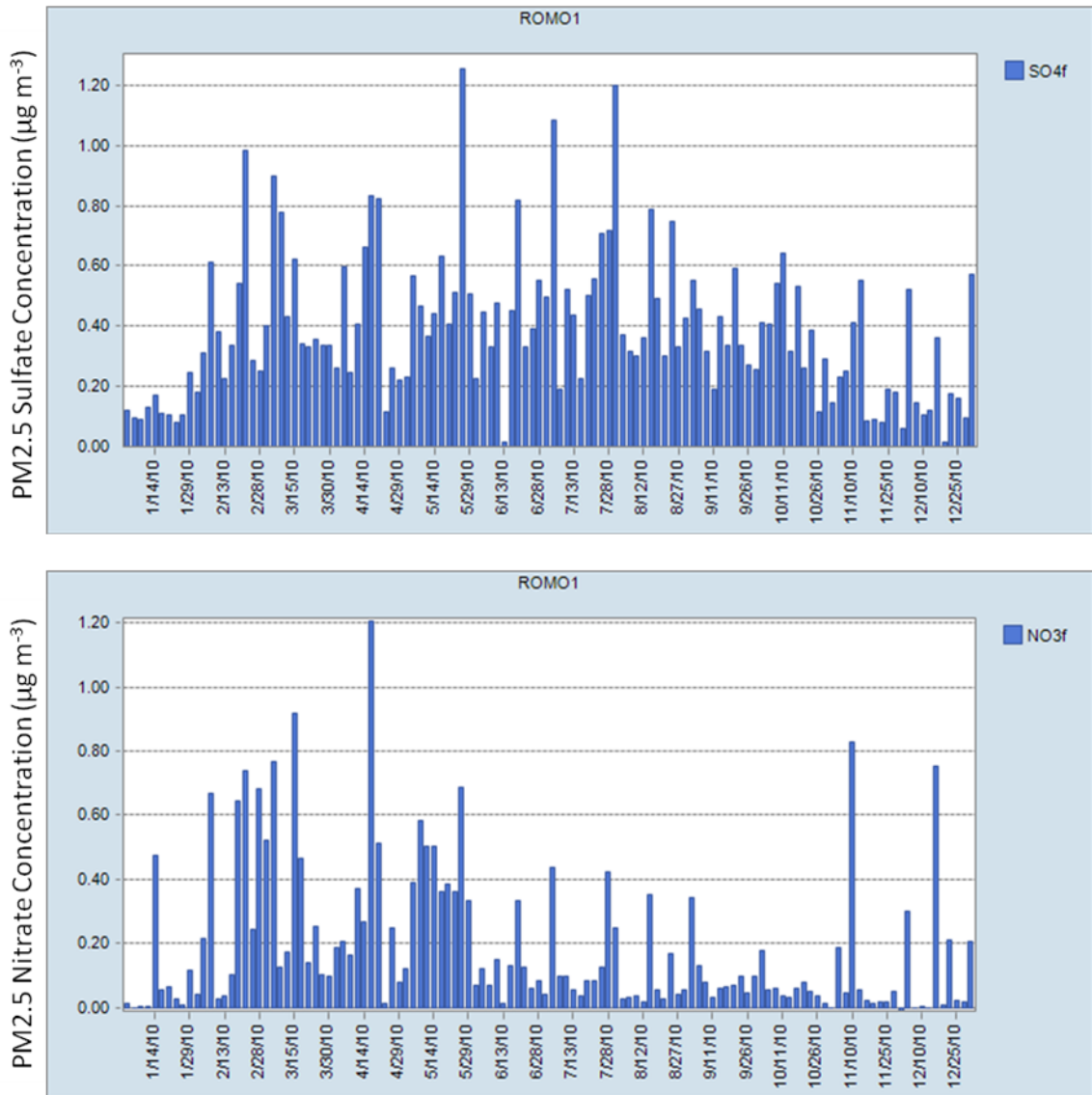


Figure 5.1: The sulfate and nitrate concentrations from 24 hour PM_{2.5} filter samples collected in RMNP during 2011 are displayed (IMPROVE, 2010).

To gain a general idea of the air quality for the sampling location in Fort Collins, Colorado, the total PM_{2.5} concentrations as measured by the Colorado Department of Public Health and Environment are shown in Figure 5.2. Over the same time period of the ACE field campaign in Fort Collins, the measured PM_{2.5} concentrations range from 0 to 15 µg m⁻³ with an average concentration of 4.7 µg m⁻³. This average is well below

the USEPA daily PM_{2.5} National Ambient Air Quality Standard of 35 $\mu\text{g m}^{-3}$ (U.S. EPA, 2009). For comparison, the average PILS sulfate and nitrate concentrations during this time period were 0.35 and 0.17 $\mu\text{g m}^{-3}$, respectively.

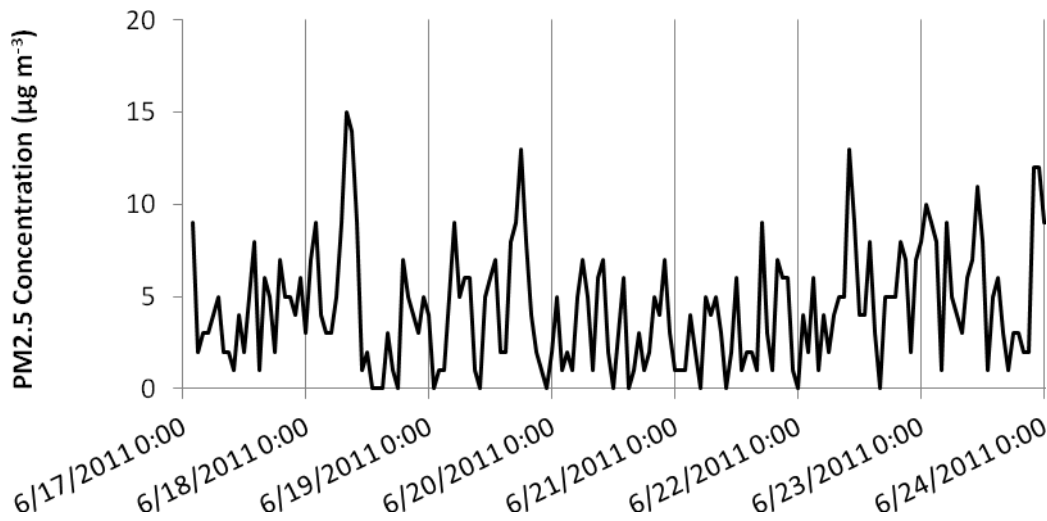


Figure 5.2: Hourly PM_{2.5} concentrations as measured by the Colorado Department of Public Health and Environment in Fort Collins at the CSU Facilities site (colorado.gov, 2011).

The sampling location for the total PM_{2.5} measurement is at the facilities site on the main campus at Colorado State University (CSU). This sampling location is in the north central area of Fort Collins. In contrast, the sulfate and nitrate concentrations measured by ACE were collected at the Department of Atmospheric Science at CSU, which is approximately 6 km northwest of the CSU facilities site. Additionally, the Atmospheric Science Department is located on the northwestern edge of the city of Fort Collins. Though the total PM_{2.5} concentration are not directly comparable to sulfate and nitrate concentrations due to the differences in sampling location and type of measurement, this

gives a general idea of the air quality at sampling location during the sampling period and that the $PM_{2.5}$ concentrations were relatively low.

5.2 Comparison of Ambient Aerosol Measurements

Calculating the percent difference between the calculated average ACE and PILS-IC concentrations gave an initial indication of the variation between these two instruments. This calculation is referred to as the overall percent difference. Averaged over the entire sampling period, the total ACE sulfate concentration is 1.8% lower and ACE nitrate concentration is 136% lower than the respective PILS-IC concentrations in RMNP. Similarly in FC, the ACE sulfate concentration is 12% higher than PILS-IC and ACE nitrate concentration is 24% higher than PILS-IC concentrations. The ACE measurements were consistently lower than the PILS measurements for both species present in the samples for RMNP but the opposite trend was observed in the concentrations measured at FC. High variability of ACE performance in different field studies is suggested by the large differences in the percent difference between each species and each field study. In RMNP, the largest discrepancy between nitrate was calculated, which corresponded with the lowest averaged measured concentration measured in either field study. Since the average concentration over the entire sampling period is used, the temporal variation is lost, so this calculation is only to gain a general assessment of the overall comparison between the average ACE and PILS-IC values.

To gain a better sense of how the ACE and PILS-IC instruments compared between each measurement, the percent difference between each PILS measurement and the averaged

ACE measurement corresponding to the PILS sample time was calculated and then averaged over the entire sampling period. This calculation is referred to as the individual percent difference. Since ACE values were both higher and lower than PILS values throughout the sampling period, the absolute value of this difference was calculated to gain a true measure of the magnitude of difference between the two instruments. In RMNP, the percent differences between the two instruments for sulfate and nitrate were 72% and 10%, respectively. The differences in the concentrations in FC were much higher. The measured sulfate concentration was 217% and nitrate concentration was 498% different between the two instruments. Compared with the overall percent difference, this calculation showed much better agreement between the RMNP nitrate values. In FC, these calculations gave significantly higher percent difference values than the overall percent difference.

To further investigate the contribution to this substantial difference in ACE and PILS-IC measurements during each sampling period, other analysis techniques were considered. Since there is significantly more uncertainty in the ACE measurements, as proven by the large relative 95% confidence intervals as shown in Table 4.2, the percent difference can most likely be attributed to the ACE measurements. Recalling the large amount of data scatter in ACE data as displayed in Figure 3.2, particularly in the FC study, also helps to confirm the ACE measurements as less reliable compared to the PILS measurements. The possible reasons for high data scatter and uncertainty in the ACE measurements are described in more detail below.

In addition to the uncertainty in the ACE measurements from the analysis technique, instrumental limitations were also considered to explain the large percent difference versus the PILS-IC measurements. Specifically, the impact of the ACE LOD on the sample measurements was investigated. As measurements near the LOD, their calculated value becomes less certain that it is representative of the true value being measured. For both FC and RMNP, the fractions of ACE concentrations that fell below the LOD were calculated. In RMNP, 97% of nitrate values and only 6% of sulfate values were below the calculated LOD. In FC, 59% of nitrate values and 34% of sulfate values were below the LOD. Particularly for nitrate measured in RMNP where almost all values were below the calculated LOD, there is much uncertainty in the validity of these measurements.

Even though the PILS is a commercial instrument used in many previous field studies, the uncertainties with the PILS measurements must also be considered. In previous studies, PILS-IC measurements have been able to reach good correlation between other instruments such as filter samples, an AMS and continuous nitrate and sulfate monitors (Hogrefe et al., 2004). However, one study has shown that sulfate can be underestimated in PILS-IC measurements (Yao et al., 2009). The potential uncertainty in PILS values was addressed by comparing with a third method of collecting sulfate and nitrate concentrations.

The URG concentrations for nitrate and sulfate, presented in Table 3.1, were also used to compare with ACE measurements at RMNP. The measured ACE concentrations were 34% and 37% higher than the measured URG filter concentrations for sulfate and nitrate,

respectively, for a three day average. For the same comparison with PILS concentrations, the averaged concentrations were 34% and 83% higher than URG filter concentrations for sulfate and nitrate, respectively. This indicates that both ACE and PILS measurements overpredict both sulfate and nitrate compared to the filter sample concentrations. However, these calculations show only a three day average, so no robust trend can be gained. Again, it should also be considered that only very low concentrations for both sulfate and nitrate were measured during this time period which makes data analysis more challenging and the measured concentrations more uncertain.

CHAPTER 6. INSTRUMENT PERFORMANCE IN FIELD OPERATION

6.1 Instrument Automation and Limitations

The inherent challenges for the successful operation of a prototype instrument combined with the challenges in running any instrument at a field site made the collection of reliable ACE measurements difficult. With the intent of keeping the ACE instrument highly automated, simple in design and robust enough for extended field operations, the system has undergone many modifications since its initial development. Many simple and temporary adjustments were performed that improved performance but did not enhance the durability of the overall instrument. Alternatively, some changes were made to improve the instrument performance in the field, but did not always work to keep the overall instrument design simple. As with any portable sampling instrument, keeping the design simple will, in general, aid in keeping the desired portability and smaller size of the ACE instrument. To best understand both the current state and the future capabilities of the ACE instrument, recent modifications and limitations to the particle collection, automation and microchip of the ACE instrument are discussed.

A significant limitation in the particle collection is the collection efficiency of the growth tube, particularly in areas with high particle concentrations. Two proposed mechanisms that act to reduce collection efficiency in high particle concentrations were previously discussed in Hering and Stolzenburg (2005). In one mechanism, as particles are being

activated, the latent heat released from condensation will alter the temperature profile in the growth tube. This will act to lower the supersaturation in the growth tube and therefore reduce collection efficiency. Another mechanism to reduce collection efficiency is that a large particle concentration will act to deplete the water vapor, which will also decrease the supersaturation within the growth tube. Of these two effects, it was shown that the depletion of water vapor was much less important than the latent heat release mechanism in reducing collection efficiency. However, high particle concentrations were not observed in either field campaign so concentrations effects were not an issue.

For extending sampling capabilities for field work, modifications were performed on ACE for increasing the automation of instrument operation. An example of one instrument alteration was the addition of flushing tubing in the sample reservoir to allow for automatic replacement of the buffer solution. This increased the time the instrument could be run without the need for any manual interference. However, initial deployment of the ACE instrument after this modification at RMNP led to instrument failure. The flushing tubing was not secured properly into the replacement buffer solution, preventing the buffer solution from being replaced each hour long cycle. This failure could have been prevented if the tubing was properly secured, showing that more attentiveness is needed to ensure proper instrument performance with this rapidly changing instrument.

Another challenge of the instrument set up has been finding a reliable method of controlling the water replacement rate of the growth tube reservoir. Currently, a syringe

pump is set at a constant rate to replace the water reservoir continuously during operation. During use, the rate of water evaporation from the growth tube depends on the temperature of the growth tube and the sample flow rate through the growth tube. This evaporation rate, assuming pure water, was estimated using the Antoine equation to find the vapor pressures at the specific temperatures of the growth tube. The calculated vapor pressure was used in a modified ideal gas law with volume and moles expressed as a rate. The growth tube sample volume flow rate was used to find the moles of water lost due to evaporation, also expressed as a rate. This molar loss rate was then converted to the rate of volume of water lost over the temperature difference of the growth tube (Noblitt, personal communication). This is a good estimate for the loss rate of water in the growth tube reservoir. However, during field studies where conditions were not constant, the loss rate was found to fluctuate and required manual adjustments to the rate of water replacement.

Temperature control of the microchip reservoir is necessary to prevent the formation of condensation in the interior of the microchip box. Condensation has been previously shown to cause arcing between the high voltage of the microchip and surrounding grounded surfaces. To prevent condensation, the temperature of the microchip box must be kept at a higher temperature than the moist air entering the microchip box from the growth tube. Once the air leaves the microchip box it comes in contact with tubing that is at room temperature and is often cooler than the microchip box temperature. The air condenses onto the inner walls of the tubing and flows into a water trap set up in the sampling line. The temperature control of the microchip box is not straightforward,

because if the temperature is increased too much, the buffer solution in the sample reservoir will dry up and prevent sample injections or alter the sample reservoir volume. The ideal temperature was often found by a trial and error approach, as the conditions varied by sample location. A new growth tube design, which features a cold, hot, and then cold temperature profile, will greatly reduce the water vapor content of air exiting the growth tube and should greatly alleviate these problems.

In addition to maintaining good temperature control of the microchip box, precise temperature control is also necessary to maintain the correct temperature range in the growth tube. In order to maintain the optimal collection efficiency, the differential temperature profile of the growth tube needs to remain above the threshold value of 27°C. With a computer program, the hot and cold temperatures are controlled to maintain at least the minimum temperature difference to guarantee the most efficient particle collection.

6.2 Challenges of the Electrophoresis Separation

The use of microchip capillary electrophoresis (MCE) has provided an additional challenge since the ACE is the first instrument to use this separation technique to measure ambient aerosol in real time. New issues arising from using MCE for ambient aerosol sampling in addition to well known issues in MCE have provided many challenges in the development of the ACE system.

Optimal microchip performance is critical to the collection of reliable data. Microchip fabrication is a very exact process with significant potential for errors. However, when microchips are made correctly, there is little variation in performance between different microchips. The soft polymer material used to make the microchips and the thin wires only micrometers in diameter make each microchip delicate and susceptible to damage during transport. Care must be taken in transporting the microchips to protect the integrity of the microwires, especially when traveling to field sites. Additionally, placing the microchip in its box before sample collection requires the high voltage power supply and ground wires to be connected directly to the chip, which can place torque on the microchip and potentially damage or break the connection with the microwires sealed in the microchip.

For the studies at RMNP and FC, two different microchips were used, but each microchip was used for the entire study. Since the microchip was not changed during sampling collection at either field study, the possibility of discrepancies between different microchips used in one field campaign was eliminated. Both in RMNP and in FC, microchip performance tended to decrease as time progressed. As an example, in RMNP, a leak developed near the flushing tubing on the underside of the sample reservoir prior to sample collection on September 17 but was able to be fixed in the field by sealing with Apiezon vacuum grease. Also in RMNP, towards the end of the sampling campaign, beginning on September 21, the microchip detection wire connection began to fail, ending the sample collection. The failing connection of the detection wires led to much higher noise values. This increased the scatter of the data points towards the end of the

sampling campaign. In FC, increased data scatter was also seen towards the end of the field campaign in the sulfate concentrations. Noise also increased in the second half of the field study making it impossible to detect nitrate. Further investigation is needed to determine the cause of the decreased microchip performance after only a few days of sampling.

The increased sensitivity of MCE separations when compared to methods using chromatography such as the PILS can make removing buffer solution or microchip contamination an increasingly hard obstacle to overcome. This issue was seen while collecting data in RMNP. A wide, negative peak due to contamination of the buffer solution, likely arising from dust contamination or human contact while handling the microchip, was present. Negative peaks could arise from contamination in the buffer solution or contamination from the reservoir surfaces of the microchip. Any detectable compound present in the buffer solution, which creates the background signal, would show up as a negative peak assuming this compound is present at lower concentrations in the injected sample. This problem may have been prevented by performing a more thorough cleaning of the microchip prior to use. The contamination peak has a migration time between 32-33 seconds which matches that of chloride. Chloride could have been transferred by touching the microchip surface. Assuming a constant contamination concentration, this amount of contamination is factored out of the ambient concentration in the differential calculation so contamination does not necessarily prevent the detection of collected sample. However, in this instance, the chloride contamination peak was large enough to interfere with the analysis of sulfate. Thus, sulfate was not able to be

analyzed during this sampling period. Additionally, higher noise during this initial sampling period along with a low nitrate signal also prevented the analysis of nitrate.

6.3 Uncertainty Analysis of ACE

The total uncertainty in the ambient aerosol measurement can be divided into components according to the ambient aerosol concentration calculation. The uncertainties are presented as the RCI. The sample volume, sample flow rate and internal standard concentration uncertainties are the same for the ACE system at each field study. The sample volume contributes 0.8%, the sample flow rate contributes 3% and the internal standard volume contributes 3.1%. The uncertainties from the aqueous concentration measurement and calibration slope differ between each field study and each aerosol component. The uncertainties for the slope in RMNP were 0.7% for sulfate and 0.6% for nitrate. In FC, the uncertainties for the slope were 0.9% from sulfate and 1.4% from nitrate. For RMNP, the uncertainties from the aqueous concentration measurement from sulfate were 50% and from nitrate were 689%. For FC, the uncertainties from sulfate were 515% and 732%. Only the uncertainty from the aqueous sample concentration has a significant impact on the total uncertainty. This motivates further investigation of the impact of the ambient aerosol calculation on the measured concentrations.

To explain how the peak areas may fluctuate from reasons other than changes in concentration, the method of separation must be considered. Separation by electrophoresis can be affected by changes in the buffer solution over time. As the ACE system is running, sample is being collected that will alter the composition of the buffer

in the sample reservoir. This is then injected into the microchip channels, and some of the ions in the sample and buffer solution can migrate towards other reservoirs according to their charge. Over time this changes the conditions of the separation and alters the voltage gradients. This phenomenon, along with fluctuating temperatures and variations in injection, can change separation properties such as the migration times and peak areas of the compounds being separated.

As an initial test, the average migration times presented in Table 6.1 as measured during the generated aerosol tests are analyzed. The range of the migration times for both sulfate and PDS from the 50 nm diameter generated aerosols was calculated to indicate how much the peak migration time shifted during the study. Looking at the generated aerosol tests only shows the effect of ammonium sulfate particles increasing at a constant rate over time on the average migration time. The range indicates how much the migration times can shift during analysis.

Table 6.1: The average migration times of sulfate and the internal standard PDS measured during the generated aerosol studies are listed for 50 nm diameter particles with the range in parenthesis.

Species	Migration Time (s)
Sulfate	29.3 (28.0-30.0)
PDS	42.9 (40.1-44.2)

Similarly, the migration times of nitrate, sulfate and PDS during the sampling at RMNP are also shown. Compared to Table 6.1, the migration times in Table 6.2 from field measurements show the effects of variable ambient aerosol on the migration time over the entire sampling period. A wider range of migration times was observed for both

sulfate and PDS during the study at RMNP compared to the generated 50 nm diameter particle tests. The range of the migration times of nitrate was found to be less than the range of migration times for sulfate in RMNP as shown in Table 6.2.

Table 6.2: The average migration times of sulfate, nitrate and PDS collected during the RMNP field campaign are listed with the range of migration times in parenthesis.

Species	Migration Time (s)
Sulfate	36.3 (35.3-40.2)
Nitrate	40.8 (39.6-43.0)
PDS	52.8 (50.9-56.5)

Since the peaks are found by finding the area under a Gaussian curve using a computer program that searches for peaks in an inputted time range, changes in peak migration time might cause the peak to fall partially out of the specified time range. Generally, the peaks that have the shortest time between them are chloride and sulfate which have a difference in migration times of about 3.5 seconds. With higher concentrations in both compounds creating a larger peak area, these peaks could easily overlap or fall out of the integration range if migration times are fluctuating over time. With peaks shifting as high as 3 seconds or more than the average migration time, such as measured in the PDS peak in RMNP, averaging the peak areas prior to integration could have a negative effect on the calculated peak area. However, each electropherogram was inspected for peak overlap and none was observed over the entire analysis period for both RMNP and FC.

To avoid any bad peak integrations, the peak definitions were manually adjusted in the peak integration program for each injection to ensure all peaks were captured. However, this integration procedure can be time intensive and a more automated method of peak integration would be desired particularly for when ACE is used for longer field studies or

if multiple ACE instruments are used in one study. To reduce peak integration errors as the procedure becomes more automated, shifts in peak migration time should be reduced.

How the peak areas of both the analyte and the internal standard change over the sampling period was investigated. Looking at one sample from the generated aerosol study, the ratio of the peak area of sulfate to the internal standard was shown over time in Figure 6.1. For comparison, the aqueous sulfate and ambient sulfate concentrations are shown over the sampling period. This was plotted to show the differences in variability over the length of the sampling period. The ratio of the peak areas of sulfate to internal standard steadily increased over time.

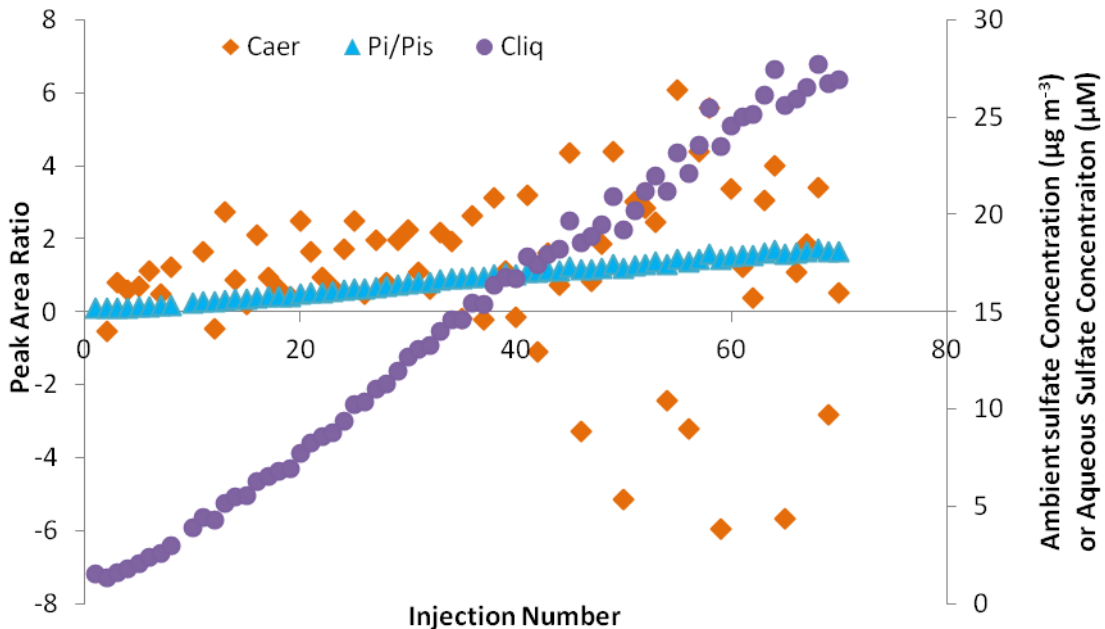


Figure 6.1: Over one injection cycle lasting 70 minutes, the ambient sulfate concentration (Caer), sulfate peak to internal standard peak ratio (Pi/Pis) and aqueous sulfate concentration (Cliq) for each 60 second analysis are plotted.

When the peak area ratios were fit with a linear trendline (not shown), the linear regression value is 0.9937, indicating a constant increase of sulfate concentration over time. The linear regression values for the aqueous sulfate concentration trend is also 0.9937. For the ambient sulfate concentration, the linear regression is 0.0002, indicating no increasing trend. This is expected since the ambient concentration of sulfate should be constant for this experiment. While the trends agree with what should be observed, the amount of data scatter in the ambient sulfate concentration is high, particularly towards the end of the sampling period. The cause of this phenomenon was investigated further.

Specifically, the differential calculation to determine the ambient concentrations may also magnify errors arising from fluctuations in the measured peak areas of both analyte and internal standard. This appears to be the case when looking at the data scatter in Figure 6.1. The highest scatter is seen in the ambient aerosol concentration whereas the data points before the ambient aerosol calculation, the peak area ratio and aqueous concentration, had much less data scatter. For example, if the internal standard peak decreased by half, the ambient aerosol concentration would increase by four times the magnitude of the previous concentration. If the internal standard peak area returned to the original value, the ambient concentration would then be four times less than the actual concentration. This creates false ambient aerosol concentrations that tend to come in consecutive pairs of values similar in magnitude but opposite in sign. Upon averaging these values, the values opposite in sign will tend to cancel, producing a value that may be closer to the accurate value.

Additionally, if ambient concentrations are near zero, the measured analyte peak will not continuously increase in size, but will stay nearly constant and fluctuate with the instrumental noise and changes in the electrophoresis separation over time. Under this condition, it is possible that the peak area will decrease slightly in size and the differential calculation to determine ambient concentration will translate this decrease into a negative concentration. The measured negative concentrations observed will increase the data scatter measured. However, boxcar averaging is generally still able to reduce the effect of negative concentrations measured on the data scatter.

It was found that the largest uncertainty in ACE measurements arises from the calculation of the aqueous concentration of the collected sample which is translated into and potentially magnified in the ambient concentration. However, though the reasons for the cause of this uncertainty were discussed, a definitive reason is not yet understood.

Variability in the peak integration procedure, internal standard and analyte peak areas measured, or the microchip electrophoresis separation over time will contribute to overall uncertainty in the ambient aerosol composition measurements. Additionally, the differential method of determining ambient aerosol concentrations in the ACE calculation, particularly in locations with low concentrations such as RMNP and FC, was shown to increase data scatter in the calculation for ambient aerosol concentrations compared to the aqueous concentration. More testing, particularly in locations with higher ambient concentrations to eliminate uncertainty from low concentrations, is needed to fully elucidate the sources of uncertainty in ACE measurements.

CHAPTER 7. CONCLUSIONS

7.1 ACE Field Study Conclusions

In this work, the ACE system was tested in two major field campaigns for instrumental performance and compared with both PILS-IC and URG filter sample measurements. These field campaigns can also be compared with a previous study performed prior to this project in Fort Collins during the summer of 2009. Along with field studies, the ACE instrument was tested in the laboratory with generated ammonium sulfate particles. This allowed the assessment of both the strengths and weaknesses of the instrument in the lab and in the field.

When the RMNP and FC field studies are compared to the previous study in Fort Collins during the summer of 2009 (FC09), some improvements were achieved but along with some shortcomings. In FC09, ACE sulfate was measured to be 19% higher than PILS measurements and ACE nitrate was 18% lower than PILS measurements. This was accomplished by averaging 3 injections for sulfate and 5 injections for nitrate. In the two field campaigns discussed in this study, ACE sulfate was 1.8% lower and 11.5% higher than PILS sulfate for RMNP and FC, respectively. For nitrate, ACE measurements were 136% lower and 23.8% higher in RMNP and FC, respectively. This was for approximately 12 injection (17 minute) averaging for both sulfate and nitrate in both studies. These differences show the discrepancies between the concentrations averaged

over the entire sampling period. This averaged concentration difference shows that the measurements of sulfate in the field campaigns at RMNP and FC were comparable to the previous ACE study, but higher discrepancies in nitrate, particularly in RMNP, could suggest poor instrument performance. However, the average concentration of nitrate at RMNP, only $0.11 \mu\text{g m}^{-3}$ as measured by the PILS, was close to the LOD of $0.09 \mu\text{g m}^{-3}$. Many of the individual measurements fell below the LOD, making this averaged value uncertain. For comparison, in FC09, $0.27 \mu\text{g m}^{-3}$ nitrate was measured.

A major achievement was the successful collection of continuous multi-day ACE measurements. Compared to the previous study in which approximately 28 hours of continuous measurements were collected, in the FC study continuous measurements for over six days was achieved. This was possible due to the improvements to instrument automation. Redesigning the microchip to decrease ion depletion, enlarging the buffer reservoirs, and adding solenoid pumps to replace the sample solution increased unattended ACE sampling time from on the order of one hour to multiple days. These improvements in instrument automation enable the ACE instrument to be used in field campaigns over long sampling periods.

Along with the increased instrument automation, the ACE system exhibited much higher data scatter than the previous study in Fort Collins. This higher data scatter was observed even with increased averaging. The exact source of this data scatter is uncertain, but it was shown that the unpredictability in instrument performance prevents the ACE instrument from consistently obtaining highly sensitive measurements with minimum

data scatter. This issue was especially apparent in the two field studies at RMNP and FC and exaggerated due to the low concentrations of both sulfate and nitrate observed. The increased noise seen during these field campaigns combined with the low signals measured made calculating the sulfate and nitrate concentrations challenging.

7.2 ACE Laboratory Study Conclusions

The initial laboratory generated aerosol tests gave good comparisons between ACE and CPC derived sulfate concentrations for 50 nm diameter particles at concentrations between 0.6 and 1.1 $\mu\text{g m}^{-3}$. The four concentrations tested showed good agreement between the ACE and CPC derived concentration measurements giving only an average 7% difference between the two measurement techniques. In contrast, the tests analyzing 30 nm or 100 nm particles had much worse agreement and motivate the need for additional testing of various particle sizes and concentrations.

CHAPTER 8. FUTURE WORK

8.1 Future Field Studies

In future field work, different sampling sites with a variety of aerosol conditions, particularly those with higher sulfate and nitrate concentrations and measureable oxalate and chloride concentrations, will be chosen for additional ACE testing. A location with higher aerosol loading will also be useful in testing the upper particle concentration limits in the new growth tube design. Additionally, locations with variable aerosol composition due to local emissions or transport would be valuable in gaining an understanding of how representative the ACE measurements are to ambient aerosol composition concentrations when they are rapidly changing.

8.2 Future Laboratory Tests

Continued laboratory testing is needed for a complete analysis with generated aerosol for ACE measurement validation. Continuing with generated ammonium sulfate particles, a larger range of particle sizes and concentrations will be tested. Additionally, particle size distributions will be measured to enable the CPC derived concentration to be determined more accurately. Additional compounds will also be investigated such as the production of nitrate from ammonium nitrate particles and oxalate from the generation of oxalic acid particles. Full ACE measurement characterization will be performed using generated particles with varying particle diameter, concentration and composition.

8.3 Future Improvements to ACE

Significant improvements and changes will be made to each component of ACE to enhance instrument performance. As described above, both a new growth tube design and new conductivity detector have been developed. The new growth tube will be able to eliminate issues due to condensation build up in the microchip box by eliminating excess water vapor from the sample flow that exits the growth tube. The new detector will improve measurement sensitivity. The detector also is significantly smaller than the current detector used, which will reduce the overall ACE footprint which is desirable for field studies. Both the new growth tube and new detector will be incorporated into the ACE system for future studies.

For the microchip, improvements will continue to be made to the electronics components to prevent noise interference, such as better insulating the wires connecting the microchip to the detection or HVPS wires. By reducing instrumental noise, the signal to noise ratio will increase and therefore improve the overall instrument sensitivity which is imperative in sampling locations with low concentrations of sulfate and nitrate as seen in RMNP and FC. Additionally, the electrophoresis separation will be improved. To complement the anion separation, a cation separation will also be used to measure the important positively charged ions in atmospheric aerosol. This separation will include ions such as ammonium, calcium and potassium. To improve the current anion separation, the separation of additional common organic acids will be investigated. Work performed by Noblitt (2011) on developing a separation for organic acid ions including formate,

fumarate, malonate, succinate and glutarate as measured in biomass burning aerosol samples will be used as a starting point for investigating the possibility of including more organic acids in the current anion separation.

The small size, excellent measurement sensitivity and fast analysis times and small power requirements make the ACE system ideal for field studies and potentially for aircraft flights. After the necessary instrument improvements for consistent and ideal operating performance is achieved, the system will be retrofitted for use on aircraft for airborne measurements. With ACE capabilities to obtain highly time resolved, sensitive aerosol composition measurements, it would be a valuable addition to many aircraft field campaigns.

After overcoming some of the discussed limitations, the ACE instrument will provide a unique semi-continuous aerosol composition monitoring technique that will be useful in a variety of atmospheric applications. With the improvements as mentioned, the ACE instrument will be valuable in gaining particle composition measurements with high temporal and spatial resolution. The sensitivity of ACE will also be beneficial in areas with low aerosol concentrations. The additional advantages of having a small size footprint and being relatively inexpensive to manufacture will make ACE an ideal instrument for both ground-based and aircraft studies.

REFERENCES

- Agarwal, J.K. and Sem, G.J., 1980. CONTINUOUS-FLOW, SINGLE-PARTICLE-COUNTING CONDENSATION NUCLEUS COUNTER. *Journal of Aerosol Science* 11 (4):343-&.
- Aitken, J., 1897. On some nuclei of cloudy condensation. *Transactions of the Royal Society of Edinburgh* XXXIX.
- Albrecht, B.A., 1989. AEROSOLS, CLOUD MICROPHYSICS, AND FRACTIONAL CLOUDINESS. *Science* 245 (4923):1227-1230.
- Beem, K.B., Raja, S., Schwandner, F.M., Taylor, C., Lee, T., Sullivan, A.P., Carrico, C.M., Mcmeeking, G.R., Day, D., Levin, E., Hand, J., Kreidenweis, S.M., Schichtel, B., Malm, W.C. and Collett, J.L., 2010. Deposition of reactive nitrogen during the Rocky Mountain Airborne Nitrogen and Sulfur (RoMANS) study. *Environmental Pollution* 158 (3):862-872.
- Colorado.Gov, 2011. Air Quality Reports, Colorado Department of Public Health and Environment, Denver, CO.
- Drewnick, F., Hings, S.S., Decarlo, P., Jayne, J.T., Gonin, M., Fuhrer, K., Weimer, S., Jimenez, J.L., Demerjian, K.L., Borrmann, S. and Worsnop, D.R., 2005. A new time-of-flight aerosol mass spectrometer (TOF-AMS) - Instrument description and first field deployment. *Aerosol Science and Technology* 39 (7):637-658.
- Felhofer, J.L., Blanes, L. and Garcia, C.D., 2010. Recent developments in instrumentation for capillary electrophoresis and microchip-capillary electrophoresis. *Electrophoresis* 31 (15):2469-2486.
- Gebhart, K.A., Schichtel, B.A., Malm, W.C., Barna, M.G., Rodriguez, M.A. and Collett Jr, J.L., 2011. Back-trajectory-based source apportionment of airborne sulfur and

nitrogen concentrations at Rocky Mountain National Park, Colorado, USA. *Atmospheric Environment* 45 (3):621-633.

Gotz, S. and Karst, U., 2007. Recent developments in optical detection methods for microchip separations. *Analytical and Bioanalytical Chemistry* 387 (1):183-192.

Guijt, R.M., Evenhuis, C.J., Macka, M. and Haddad, P.R., 2004. Conductivity detection for conventional and miniaturised capillary electrophoresis systems. *Electrophoresis* 25 (23-24):4032-4057.

Hand, J.L., 2011. Spatial and Seasonal Patterns and Temporal Variability of Haze and its Constituents in the United States. Report V (0737-5352-87).

Hartonen, K., Laitinen, T. and Riekkola, M.L., 2011. Current instrumentation for aerosol mass spectrometry. *Trac-Trends in Analytical Chemistry* 30 (9):1486-1496.

Hering, S.V., Collett, J.L. and Henry, C.S., 2009. A compact, in-situ instrument for organic acid aerosols, DOE STTR Phase II Grant, 101.

Hering, S.V. and Stolzenburg, M.R., 2005. A method for particle size amplification by water condensation in a laminar, thermally diffusive flow. *Aerosol Science and Technology* 39:428-436.

Hogrefe, O., Schwab, J.J., Drewnick, F., Lala, G.G., Peters, S., Demerjian, K.L., Rhoads, K., Felton, H.D., Rattigan, O.V., Husain, L. and Dutkiewicz, V.A., 2004. Semicontinuous PM_{2.5} sulfate and nitrate measurements at an urban and a rural location in New York: PMTACS-NY summer 2001 and 2002 campaigns. *Journal of the Air & Waste Management Association* 54 (9):1040-1060.

Improve, 2010. The Visibility Information Exchange Web System (VIEWS).

Ippc, 2007. Contribution of Working Groups I, II, and III to the Fourth Assessment Report of the Intergovernmental Panel on Climate Change, in *Climate Change 2007: Synthesis Report*, Core Writing Team, R.K. Pachauri and A. Reisinger, eds., Geneva, Switzerland, 104.

Jayne, J.T., Leard, D.C., Zhang, X., Davidovits, P., Smith, K.A., Kolb, C.E. and Worsnop, D.R., 2000. Development of an Aerosol Mass Spectrometer for Size

and Composition Analysis of Submicron particles. *Aerosol Science and Technology* 33:49-70.

Khlystov, A., Wyers, G.P. and Slanina, J., 1995. The steam-jet aerosol collector. *Atmospheric Environment* 29 (17):2229-2234.

Kucienska, B., 2009. A simulation of the influence of organic and inorganic pollutants on the formation and development of warm clouds over Mexico City. *Atmospheric Research* 95 (4):487-495.

Lavery, T.F., Rogers, C.M., Baumgardner, R. and Mishoe, K.P., 2009. Intercomparison of Clean Air Status and Trends Network Nitrate and Nitric Acid Measurements with Data from Other Monitoring Programs. *Journal of the Air & Waste Management Association* 59 (2):214-226.

Lee, T., Yu, X.-Y., Kreidenweis, S.M., Malm, W.C. and Collett, J.L., 2008. Semi-continuous measurement of PM_{2.5} ionic composition at several rural locations in the United States. *Atmospheric Environment* 42:6655-6669.

Liu, P., Ziemann, P.J., Kittelson, D.B. and McMurry, P.H., 1995. Generating Particle Beams of Controlled Dimensions and Divergence: I. Theory of Particle Motion in Aerodynamic Lenses and Nozzle Expansions. *Aerosol Science and Technology* 22 (3):293-313.

Liu, Y., Fanguy, J.C., Bledsoe, J.M. and Henry, C.S., 2000. Dynamic coating using polyelectrolyte multilayers for chemical control of electroosmotic flow in capillary electrophoresis microchips. *Analytical Chemistry* 72 (24):5939-5944.

Mader, B.T., Yu, J.Z., Xu, J.H., Li, Q.F., Wu, W.S., Flagan, R.C. and Seinfeld, J.H., 2004. Molecular composition of the water-soluble fraction of atmospheric carbonaceous aerosols collected during ACE-Asia. *J. Geophys. Res.* 109 (D6):D06206.

McMurry, P.H., Shepherd, M.F., Vickery, J.S. and Narsto, 2004. *Particulate matter science for policy makers: a NARSTO assessment*. Cambridge University Press

Noble, C.A. and Prather, K.A., 1996. Real-time measurement of correlated size and composition profiles of individual atmospheric aerosol particles. *Environmental Science & Technology* 30 (9):2667-2680.

- Noblitt, S.D., 2011. Development of a microchip electrophoresis system for online monitoring of atmospheric aerosol composition. Doctor of Philosophy, Colorado State University, Fort Collins.
- Noblitt, S.D. and Henry, C.S., 2008. Improving the compatibility of contact conductivity detection using microchip electrophoresis using a bubble cell. *Analytical Chemistry* 80:7.
- Noblitt, S.D., Lewis, G.S., Lui, Y., Hering, S.V., Collett, J.L. and Henry, C.S., 2009a. Interfacing microchip electrophoresis to a growth tube particle collector for semicontinuous monitoring of aerosol composition. *Analytical Chemistry* 81:9.
- Noblitt, S.D., Schwandner, F.M., Hering, S.V., Collett, J.L. and Henry, C.S., 2009b. High-sensitivity microchip capillary electrophoresis determination of inorganic anions and oxalate in atmospheric aerosols with adjustable selectivity and conductivity detection. *Journal of Chromatography A* 1216:8.
- Orsini, D.A., Ma, Y., Sullivan, A., Sierau, B., Baumann, K. and Weber, R.J., 2003. Refinements to the particle-into-liquid sampler (PILS) for ground and airborne measurements of water soluble aerosol composition. *Atmospheric Environment* 37:17.
- Pope, C.A. and Dockery, D.W., 2006. Health Effects of Fine Particulate Air Pollution: Lines that Connect. *Air and Waste Management* 56:709-742.
- Prather, K.A., Hatch, C.D. and Grassian, V.H., 2008. Analysis of Atmospheric Aerosols. *Annual Review of Analytical Chemistry* 1:485-514.
- Pu, Q.S., Yun, J.S., Temkin, H. and Liu, S.R., 2004. Ion-enrichment and ion-depletion effect of nanochannel structures. *Nano Letters* 4 (6):1099-1103.
- Ramanathan, V., Crutzen, P.J., Kiehl, J.T. and Rosenfeld, D., 2001. Aerosols, Climate, and the Hydrological Cycle. *Science* 294:2119-2124.
- Rompp, A., Winterhalter, R. and Moortgat, G.K., 2006. Oxodicarboxylic acids in atmospheric aerosol particles. *Atmospheric Environment* 40 (35):6846-6862.

- Rosenfeld, D., 1999. TRMM observed first direct evidence of smoke from forest fires inhibiting rainfall. *Geophysical Research Letters* 26 (20):3105-3108.
- Schlesinger, R.B., 2007. The health impact of common inorganic components of fine particulate matter (PM_{2.5}) in ambient air: A critical review. *Inhalation Toxicology* 19 (10):811-832.
- Seinfeld, J.H. and Pandis, S.N., 2006. *Atmospheric chemistry and physics: from air pollution to climate change*. Wiley
- Sickles, J.E. and Shadwick, D.S., 2008. Comparison of particulate sulfate and nitrate at collocated CASTNET and IMPROVE sites in the eastern US. *Atmospheric Environment* 42 (9):2062-2073.
- Skoog, D.A., Holler, J.F. and Crouch, S.R., 2007. *Instrumental Analysis*. Brooks/Cole, New Dehli
- Slanina, J., Ten Brink, H.M., Otjes, R.P., Even, A., Jongejan, P., Khlystov, A., Waijers-Ijpelaan, A. and Hu, M., 2001. The continuous analysis of nitrate and ammonium in aerosols by the steam jet aerosol collector (SJAC): extension and validation of the methodology. *Atmospheric Environment* 35 (13):2319-2330.
- Sullivan, R.C., 2005. Recent advances in our understanding of atmospheric chemistry and climate made possible by on-line aerosol analysis instrumentation. *Analytical Chemistry* 77:3861-3886.
- Ten Brink, H., Otjes, R., Jongejan, P. and Kos, G., 2009. Monitoring of the ratio of nitrate to sulphate in size-segregated submicron aerosol in the Netherlands. *Atmospheric Research* 92 (2):270-276.
- Trebs, I., Meixner, F.X., Slanina, J., Otjes, R., Jongejan, P. and Andreae, M.O., 2004. Real-time measurements of ammonia, acidic trace gases and water-soluble inorganic aerosol species at a rural site in the Amazon Basin. *Atmospheric Chemistry and Physics* 4:967-987.
- Twomey, S., 1974. POLLUTION AND PLANETARY ALBEDO. *Atmospheric Environment* 8 (12):1251-1256.
- U.S. Epa, 2009. Integrated Science Assessment for Particulate Matter (Final Report), U.S. Environmental Protection Agency, ed., Washington, DC.

Weber, R., Orsini, D.A., Daun, Y., Lee, Y.-N., Klotz, P.J. and Brechtel, F., 2001. A particle-into-liquid collector for rapid measurement of aerosol bulk chemical composition. *Aerosol Science and Technology* 35:10.

Yao, X., Shairsing, K., Lam, P.H. and Evans, G., 2009. Underestimation of sulfate concentration in PM_{2.5} using a semi-continuous particle instrument based on ion chromatography. *Journal of Environmental Monitoring* 11:1292-1297.